Spatial Movement with Distributed Memory*

Qingyan Shi[1], Junping Shi[2†], Hao Wang[3]

[1] School of Science, Jiangnan University, Wuxi, Jiangsu, 214122, China.

Email: qingyanshi@jiangnan.edu.cn

[2] Department of Mathematics, William & Mary, Williamsburg, VA, 23187-8795, USA.

Email: jxshix@wm.edu

[3] Department of Mathematical and Statistical Sciences, University of Alberta,

Edmonton, AB T6G 2G1, Canada.

Email: hao8@ualberta.ca

Abstract

Diffusion has been widely applied to model animal movements following Brownian motions. However, animals typically move like non-Brownian motions due to their perceptual judgement. Spatial memory and cognition have recently received much attention in characterizing the collective animal movement behaviors. Explicit spatial memory is modeled via a distributed delayed diffusion term in this paper. The distributed time represents the memory gaining and waning over time, and the distributed space represents the dependence of spatial memory over locations. When the temporal delay kernel takes the weak kernel, the equation is equivalent to a Keller-Segel chemotaxis model. When the temporal delay kernel takes the strong kernel, the equation has both steady state bifurcation and spatially non-homogeneous Hopf bifurcation, which lead to rich spatiotemporal patterns.

Keywords: spatial memory; reaction-diffusion equation; distributed delayed diffusion; pattern formation; spatially non-homogeneous time periodic solution; Hopf bifurcation; Turing bifurcation

MSC2000: 34K18, 92B05, 35B32, 35K57

*Partially supported by a grant from China Scholarship Council, US-NSF grant DMS-1715651, and an NSERC grant.

†Corresponding Author

1 Introduction

Diffusion equation has been popularly used to model random movements of both macroscopic and microscopic substances. While in general diffusion has an averaging and smoothing effect on the distribution of density function, different diffusion rates of different species may lead to spatial pattern formation as a result of Turing instability [35]. However in the natural world, the spatial movement of organisms or animals is the collective behaviors of non-Brownian motions. It has been recognized that the episodic-like spatial memory and cognition are important factors for determining animals' diffusive movement with bias [10].

Here we formulate a partial differential equation model for a single species animal movement in the explicit incorporation of spatial memory via a distributed spatiotemporal delayed diffusion. Let $u(x,t)$ be the population density of an animal species in spatial location x at time t. We assume that the population is in a spatial habitat Ω, an open, bounded and connected subset of $\mathbb{R}^m$ with $m = 1, 2, 3$, and the boundary $\partial\Omega$ is smooth. The population density $u(x,t)$ satisfies

$$\begin{cases} u_t(x,t) = d_1\Delta u(x,t) + d_2 div(u(x,t)\nabla v(x,t)) + f(u(x,t)), & x \in \Omega,\ t > 0, \\ \partial_n u(x,t) = 0, & x \in \partial\Omega,\ t > 0, \\ u(x,t) = \eta(x,t), & x \in \Omega,\ t \in (-\infty, 0], \end{cases} \tag{1.1}$$

where the function $v(x,t)$ is defined by

$$v(x,t) = g * *u(x,t) = \int_{-\infty}^{t}\int_{\Omega} G(x,y,t-s)g(t-s)u(y,s)dyds; \tag{1.2}$$

the parameters $d_1 > 0$ and $d_2 \in \mathbb{R}$ are the random diffusion coefficient and the memory-based diffusion coefficient respectively; the function f describes the chemical reaction or biological birth/death of the population; the function $u(x,t)$ satisfies a no-flux boundary condition so the system is a closed one ($\partial_n u$ is the outer normal derivative of u at $x \in \partial\Omega$). In (1.2), the spatiotemporal averaging kernel function $G(x,y,t)$ is the probability that an individual in location y moves to location x at the time t, and the temporal weighing function $g(t)$ shows the distribution of dependence of memory on the past time t. Here $G : \Omega \times \Omega \times (0,\infty) \to \mathbb{R}$ is a (generalized) function or measure and $g : [0,\infty) \to \mathbb{R}^+$ is a probability distribution function satisfying

$$\int_{\Omega} G(x,y,t)dy = 1,\ \ x \in \Omega,\ t > 0, \quad \text{and} \quad \int_0^{\infty} g(t)dt = 1. \tag{1.3}$$

Hence the function $v(x,t)$ is a spatiotemporal average of the population density in the past, and it is reasonable to call $v(x,t)$ the memory function at the population in spatial location

x at time t. Such kind of nonlocal delay $v(x,t)$ was first used in [4] for an unbounded domain and in [12] for bounded domain. See also [5, 41, 42] for the direction of nonlocal delay. However, in all existing work the nonlocal delay always appears in the reaction term (growth, etc.) of the population, while in our model (1.1), the nonlocal delay appears in the spatial movement of the population. This is novel in the perspectives of both biology and mathematics.

Because of the diffusive nature of the population movement, the spatiotemporal kernel function $G(x,y,t)$ is chosen as the Green's function of diffusion equation with no-flux boundary condition, which is

$$G(x,y,t)=\sum_{n=0}^{\infty}e^{-d_1\lambda_n t}\phi_n(x)\phi_n(y), \tag{1.4}$$

where λ_n satisfying $0=\lambda_0<\lambda_1\le\lambda_2\le\cdots\le\lambda_n\le\cdots\to+\infty$, as $n\to\infty$, are the eigenvalues of the eigenvalue problem

$$\begin{cases}-\Delta u(x)=\lambda u(x), & x\in\Omega,\\ \partial_n u(x)=0, & x\in\partial\Omega,\end{cases} \tag{1.5}$$

and $\phi_n(x)$ are the corresponding eigenfunctions of λ_n normalized so that (1.3) is satisfied. Equivalently the function $G(x,y,t)$ satisfies (for fixed y)

$$\begin{cases}G_t(x,y,t)=d_1\Delta_x G(x,y,t), & x\in\Omega,\ t>0,\\ \partial_n G(x,y,t)=0, & x\in\partial\Omega,\ t>0,\\ G(x,y,0)=\delta(x-y).\end{cases}$$

Here $\delta(x)$ is the Dirac delta measure on Ω. On the other hand, a common choice of the temporal kernel function is the Gamma distribution function of order n (with $n\in\mathbb{N}\cup\{0\}$):

$$g_n(t)=\frac{t^n e^{-t/\tau}}{\tau^{n+1}\Gamma(n+1)}. \tag{1.6}$$

In particular, we mainly consider the following two specific cases which are commonly employed in the biological modeling:

$$g_0(t)=g_w(t)=\frac{1}{\tau}e^{-\frac{t}{\tau}},\quad g_1(t)=g_s(t)=\frac{t}{\tau^2}e^{-\frac{t}{\tau}}. \tag{1.7}$$

which are referred as the weak kernel and strong kernel respectively. The mean and variance of $g_n(\cdot)$ are given by $\mathbb{E}(g_n(\cdot))=(n+1)\tau$ and $\mathbb{V}ar(g_n(\cdot))=(n+1)\tau^2$, hence τ represents the average time delay kernel. The weak kernel only captures memory waning over time, while the strong kernel captures both memory gaining and memory waning over time.

The movement of the population in (1.1)-(1.2) can be derived from mass conservation law and a modified Fick's law following [31]:

$$\mathbf{J}(x,t) = -d_1 \nabla_x u(x,t) - d_2 \mathbf{w}(x,t) \cdot u(x,t),$$

where $\mathbf{w}(x,t)$ is a vector field indicating the fluid flow. In (1.1), we assume that

$$\mathbf{w}(x,t) = \nabla_x \left(\int_{-\infty}^{t} \int_{\Omega} G(x,y,t-s) g(t-s) u(y,s) dy ds \right).$$

That is, in addition to the random passive diffusion with coefficient d_1, the flux is proportional to the negative gradient of a weighted average historic density distribution. In [31] and [30], it is assumed that

$$\mathbf{w}(x,t) = \nabla_x u(x, t-\tau),$$

which indicates the flux is proportional to the negative gradient of historic density function at a fixed past time. Using a nonlocal and temporal distributed average of historic density is more realistic to reflect the fact that the waning of spatial memories is over both time and the distance of past animal distributions from the decision-making animal.

In this paper the dynamic properties and pattern formation mechanisms of (1.1)-(1.2) are extensively studied via bifurcation analysis. In particular we are interested in the question that under what conditions on the diffusion coefficients and kernel functions, the spatial patterns (non-constant steady state) or spatiotemporal patterns (spatially non-homogeneous time periodic orbits) can be generated by the system (1.1)-(1.2). When the spatiotemporal kernel function $G(x,y,t)$ is given by (1.4) and the delay distribution function $g(t)$ is given by (1.7), system (1.1)-(1.2) is equivalent to a system of two or three reaction-diffusion equations with a chemotactic term [12, 41]. For example, with the weak kernel $g_w(t)$, the equation of u in (1.1) with v given by (1.2) is equivalent to a system of two reaction-diffusion equations:

$$\begin{cases} u_t(x,t) = d_1 \Delta u(x,t) + d_2 div(u(x,t) \nabla v(x,t)) + f(u(x,t)), & x \in \Omega,\ t > 0, \\ v_t(x,t) = d_1 \Delta v(x,t) + \frac{1}{\tau}(u(x,t) - v(x,t)), & x \in \Omega,\ t > 0, \\ \partial_n u(x,t) = \partial_n v(x,t) = 0, & x \in \partial\Omega,\ t > 0. \end{cases} \tag{1.8}$$

Our theoretical results on the pattern formation are mainly derived from the bifurcation theory for the equivalent system (1.8) and also the corresponding one for the strong kernel, which are better developed. It is also a surprising coincidence that system (1.8) is the same as a rescaled Keller-Segel chemotaxis model with growth [3, 13, 15, 34]:

$$\begin{cases} u_t(x,t) = d_1 \Delta u(x,t) + d_2 div(u(x,t) \nabla v(x,t)) + f(u(x,t)), & x \in \Omega,\ t > 0, \\ v_t(x,t) = d_3 \Delta v(x,t) + a u(x,t) - b v(x,t), & x \in \Omega,\ t > 0, \\ \partial_n u(x,t) = \partial_n v(x,t) = 0, & x \in \partial\Omega,\ t > 0. \end{cases} \tag{1.9}$$

Typically $u(x,t)$ in (1.9) is the population density of cells, and $v(x,t)$ is the density of a chemical signaling molecule. When the growth function $f(u) = 0$, then Eq. (1.9) is the so-called minimum Keller-Segel model proposed by the seminal work of Keller and Segel [15].The dynamics of (1.9) with growth rate has been studied in, for example, [37–40]. The chemotaxis coefficient d_2 in the original Keller-Segel model is negative since cells are usually attracted to the higher density location of the chemical signals, but repulsive chemotaxis effect (with positive d_2) has also been considered [33, 36]. The above discussion provides an alternative derivation of the Keller-Segel chemotaxis model but the variable v is now interpreted as the "memory" which is a nonlocal and temporal distributed average of historic density, instead of as a current chemical signaling function in the classical Keller-Segel model. On the other hand, our new model based on nonlocal delayed memory can also be understood as a chemotaxis model in which the population is either attracted to ($d_2 < 0$) or repelled by ($d_2 > 0$) its past tracks. Naturally animals escape from high density due to the limitation of resources, that is, $d_2 > 0$. Some social animals have aggregations, such as starling flocks and insects, in the purpose of group defense or group working, and this collective behavior will lead to $d_2 < 0$. Potentially some animals may use optimal mixed strategies of social behaviors according to the environmental conditions, for instance, they may select to move to higher density this time when resources are abundant and they need to work together, but they may select to move to lower density next time when resources are limiting. In this case we have the switching between $d_2 > 0$ and $d_2 < 0$ when some environmental conditions change. However, we shall not consider such generalizations here, and for convenience we focus on pure strategies where d_2 attains a constant.

Throughout the paper, we assume that the nonlinear function f and diffusion coefficients satisfy

(H1) $f : U \to \mathbb{R}$ is continuously differentiable, where U is an open interval; and there exists $\theta \in U$ such that $f(\theta) = 0$ and $f'(\theta) < 0$;

(H2) $d_1 > 0$, $d_2 \in \mathbb{R}$.

Our main interest is on the stability of the constant equilibrium $u = \theta$ with respect to (1.9) (or the equivalent system), and the instability often leads to the existence of spatial or spatiotemporal patterns. Our main results can be summarized as follows:

1. for the weak kernel case: there exists $d_2^* < 0$ such that the constant equilibrium is locally asymptotically stable when $d_2 \geq d_2^*$, and it is unstable when $d_2 < d_2^*$. Moreover

steady state bifurcations occur at a sequence $d_2 = d_{2,n}^w \leq d_2^*$ to give rise to spatial patterns;

2. for the strong kernel case: there exist $d_{2,S}^* < 0$ and $d_{2,H}^* > 0$ such that

   (a) when $d_{2,S}^* \leq d_2 \leq d_{2,H}^*$, the constant equilibrium is locally asymptotically stable;

   (b) when $d_2 > d_{2,H}^*$, the constant equilibrium is unstable, and a family of Hopf bifurcation occur at $d_2 > d_{2,H}^*$ and spatially non-homogeneous periodic orbits arise;

   (c) when $d_2 < d_{2,S}^*$, the constant equilibrium is unstable, and a family of steady state bifurcations occur at $d_2 < d_{2,S}^*$ and spatially non-homogeneous steady states arise.

These results are similar to Turing diffusion-induced instability in the sense that the non-homogenous patterns are results of linear instability of constant equilibrium, but here in the strong kernel case, a large repulsive memory-based movement can also produce time-periodic patterns which does not happen for Turing mechanism. The results above also reveal the subtle difference of the weak and strong kernels on the pattern formation: for both weak and strong kernels, a large attractive memory-based movement induces spatial patterns; but only for the strong kernel, a large repulsive memory-based movement can induce spatiotemporal patterns through Hopf bifurcations. It should be noted that the weak kernel case (Keller-Segel chemotaxis model with growth) has been studied extensively in recent years [16, 20, 21, 25, 34]. Not only non-homogeneous steady state solutions have been found analytically through bifurcation methods, but non-homogenous periodic orbits and even chaotic dynamics have also been found numerically [16, 25]. Here we rigorously show the existence of spatial and temporal doubly-periodic orbits (checker board patterns) for the strong kernel and repulsive case, which is also interesting for the chemotaxis model as repulsive chemotaxis is usually thought to be a stabilizing force [33, 36]. Spatially non-homogeneous time-periodic orbits for chemotaxis models were also found in [19] for a attractive-repulsive Keller-Segel model.

This paper is organized as follows. We derive the equivalent systems of Eq. (1.1) for the weak and strong kernel cases respectively in Section 2. In Section 3, for the weak kernel case, we study the stability of the constant equilibrium of the equivalent system and provide a detained bifurcation analysis as well as the conditions for pattern formation. The bifurcation analysis of the strong kernel case is given in Section 4. We apply our general results to a logistic growth model in Section 5 and the bifurcation direction and stability of the steady state are determined. Finally, we conclude and discuss our work in Section 6 and pose some detailed calculations in Appendix.

In the paper the space of measurable functions for which the p-th power of the absolute value is Lebesgue integrable defined on a bounded and smooth domain $\Omega \subseteq \mathbb{R}^m$ is denoted by $L^p(\Omega)$ and we use $W^{k,p}(\Omega)$ to denote the real-valued Sobolev space based on $L^p(\Omega)$ space. Denote $X = \{u \in W^{2,p}(\Omega) : \partial_n u = 0,\ x \in \partial\Omega\}$ and $Y = L^p(\Omega)$, where $p > m$. We denote by $\mathbb{N}$ the set of all the positive integers, and $\mathbb{N}_0 = \mathbb{N} \cup \{0\}$.

2 Equivalence of systems

In this section, we establish the equivalence between the scalar equation (1.1) and chemotactic-diffusive systems without nonlocal delay. By the similar method in Theorems 2.3 and 2.4 in [41], we have the following results on the equivalence of the two systems under weak or strong kernel.

Lemma 2.1. *Suppose that kernel $g(t)$ is given by the weak kernel function $g_w(t) = \frac{1}{\tau}e^{-\frac{t}{\tau}}$, and define*

$$v(x,t) = (g_w * *u)(x,t) = \int_{-\infty}^{t}\int_{\Omega} G(x,y,t-s)g_w(t-s)u(y,s)dyds.$$

1. *If $u(x,t)$ is the solution of (1.1), then $(u(x,t),v(x,t))$ is the solution of*

$$\begin{cases} u_t(x,t) = d_1\Delta u(x,t) + d_2 div(u(x,t)\nabla v(x,t)) + f(u(x,t)), & x \in \Omega,\ t > 0, \\ v_t(x,t) = d_1\Delta v(x,t) + \frac{1}{\tau}(u(x,t) - v(x,t)), & x \in \Omega,\ t > 0, \\ \partial_n u(x,t) = \partial_n v(x,t) = 0, & x \in \partial\Omega,\ t > 0, \\ u(x,0) = \eta(x,0), & x \in \Omega, \\ v(x,0) = \frac{1}{\tau}\int_{-\infty}^{0}\int_{\Omega} G(x,y,-s)e^{\frac{s}{\tau}}\eta(y,s)dyds, & x \in \Omega. \end{cases} \tag{2.1}$$

2. *If $(u(x,t),v(x,t))$ is a solution of*

$$\begin{cases} u_t(x,t) = d_1\Delta u(x,t) + d_2 div(u(x,t)\nabla v(x,t)) + f(u(x,t)), & x \in \Omega,\ t \in \mathbb{R}, \\ v_t(x,t) = d_1\Delta v(x,t) + \frac{1}{\tau}(u(x,t) - v(x,t)), & x \in \Omega,\ t \in \mathbb{R}, \\ \partial_n u(x,t) = \partial_n v(x,t) = 0, & x \in \partial\Omega,\ t \in \mathbb{R}. \end{cases} \tag{2.2}$$

Then $u(x,t)$ satisfies Eq. (1.1) such that $\eta(x,s) = u(x,s)$ for $-\infty < s < 0$. In particular, if $(u(x),v(x))$ is a steady state solution of (2.2), then $u(x)$ is a steady state solution of (1.1); and if $(u(x,t),v(x,t))$ is a periodic solution of (2.2), then $u(x,t)$ is a periodic solution of (1.1).

For the strong kernel case, we can similarly obtain the following equivalence.

Lemma 2.2. *Suppose that kernel $g(t)$ is given by the strong kernel function $g_s(t) = \frac{t}{\tau^2}e^{-\frac{t}{\tau}}$, and define*

$$v(x,t) = g_s * *u(x,t) = \int_{-\infty}^{t}\int_{\Omega} G(x,y,t-s)g_s(t-s)u(y,s)dyds.$$

1. *If $u(x,t)$ is the solution of (1.1), then $(u(x,t),v(x,t),w(x,t))$ is the solution of*

$$\begin{cases} u_t(x,t) = d_1\Delta u(x,t) + d_2 div(u(x,t)\nabla v(x,t)) + f(u(x,t)), & x\in\Omega,\ t>0,\\ v_t(x,t) = d_1\Delta v(x,t) + \frac{1}{\tau}(w(x,t)-v(x,t)), & x\in\Omega,\ t>0,\\ w_t(x,t) = d_1\Delta w(x,t) + \frac{1}{\tau}(u(x,t)-w(x,t)), & x\in\Omega,\ t>0,\\ \partial_n u(x,t) = \partial_n v(x,t) = \partial_n w(x,t) = 0, & x\in\partial\Omega,\ t>0,\\ u(x,0) = \eta(x,0), & x\in\Omega,\\ v(x,0) = \int_{-\infty}^{0}\int_{\Omega} G(x,y,-s)\frac{-s}{\tau^2}e^{\frac{s}{\tau}}\eta(y,s)dyds, & x\in\Omega,\\ w(x,0) = \int_{-\infty}^{0}\int_{\Omega} G(x,y,-s)\frac{1}{\tau}e^{\frac{s}{\tau}}\eta(y,s)dyds, & x\in\Omega. \end{cases} \tag{2.3}$$

2. *If $(u(x,t),v(x,t),w(x,t))$ is a solution of*

$$\begin{cases} u_t(x,t) = d_1\Delta u(x,t) + d_2 div(u(x,t)\nabla v(x,t)) + f(u(x,t)), & x\in\Omega,\ t\in\mathbb{R},\\ v_t(x,t) = d_1\Delta v(x,t) + \frac{1}{\tau}(w(x,t)-v(x,t)), & x\in\Omega,\ t\in\mathbb{R},\\ w_t(x,t) = d_1\Delta w(x,t) + \frac{1}{\tau}(u(x,t)-w(x,t)), & x\in\Omega,\ t\in\mathbb{R},\\ \partial_n u(x,t) = \partial_n v(x,t) = \partial_n v(x,t) = 0, & x\in\partial\Omega,\ t\in\mathbb{R}, \end{cases} \tag{2.4}$$

Then $u(x,t)$ satisfies Eq. (1.1) with the strong kernel $g_s(t)$ such that $\eta(x,s) = u(x,s)$ for $-\infty < s < 0$. In particular, if $(u(x),v(x),w(x))$ is a steady state solution of (2.4), then $u(x)$ is a steady state solution of (1.1); if $(u(x,t),v(x,t),w(x,t))$ is a periodic solution of (2.4), then $u(x,t)$ is a periodic solution of (1.1).

From Lemmas 2.1 and 2.2, one can see that the existence of the steady state and periodic solutions of Eq. (1.1) with Gamma temporal distribution function and diffusion spatiotemporal kernel function. Next we show the equivalence of the stability of the constant equilibrium with respect to the two systems. From the assumption (H1), Eq. (1.1) has a positive constant equilibrium $u = \theta$. The linearization of Eq. (1.1) at $u = \theta$ is

$$\begin{cases} \psi_t(x,t) = d_1\Delta\psi(x,t) + d_2\theta\Delta\left(\int_{\Omega}\int_{-\infty}^{t} G(x,y,t-s)g(t-s)\psi(y,s)dyds\right) \\ \qquad\qquad + f'(\theta)\psi, & x\in\Omega,\ t>0,\\ \partial_n\psi(x,t) = 0, & x\in\partial\Omega,\ t>0. \end{cases} \tag{2.5}$$

By assuming that $\psi(x,t) = e^{\mu t}\varphi(x)$, the eigenvalue problem of Eq. (2.5) is given by

$$\mu\varphi = d_1\Delta\varphi + d_2\theta\Delta\left(\int_\Omega\int_{-\infty}^{t} G(x,y,t-s)g(t-s)e^{\mu s}\varphi(y)dyds\right) + f'(\theta)\varphi, \tag{2.6}$$

where $\mu \in \mathbb{C}$ and $\varphi \in X\backslash\{0\}$.

Lemma 2.3. *$\mu \in \mathbb{C}$ is an eigenvalue of Eq. (2.6) if and only if there exist some $n \in \mathbb{N}_0$ such that μ is a root of the following equation:*

$$\mu + d_1\lambda_n + \frac{d_2\theta\lambda_n}{(1 + d_1\lambda_n\tau + \mu\tau)^{m+1}} - f'(\theta) = 0, \tag{2.7}$$

where $m = 0$ for weak kernel and $m = 1$ for strong kernel.

Proof. We take the weak kernel as example to demonstrate the calculation. First, we substitute (1.4), (1.7) and $\varphi(x) = \phi_n(x)$ into Eq. (2.6) and obtain

$$\begin{aligned}
\mu\phi_n(x)e^{\mu t} &= -d_1\lambda_n\phi_n(x)e^{\mu t} + \frac{d_2\theta}{\tau}\left(\int_\Omega\int_{-\infty}^{t}\sum_{n=1}^{\infty} e^{-d_1\lambda_n(t-s)}\phi_n(x)\phi_n^2(y)e^{-(t-s)/\tau}e^{\mu s}dyds\right) \\
&\quad - f'(\theta)\phi_n(x)e^{\mu t} \\
&= -d_1\lambda_n\phi_n(x)e^{\mu t} + \frac{d_2\theta}{\tau}\int_{-\infty}^{0} e^{(d_1\lambda_n+1/\tau)s}e^{\mu s}ds\int_\Omega\phi_n^2(y)dy\phi_n(x)e^{\mu t} - f'(\theta)\phi_n(x)e^{\mu t} \\
&= -d_1\lambda_n\phi_n(x)e^{\mu t} + \frac{d_2\theta}{1 + d_1\lambda_n\tau_\mu\tau}\phi_n(x)e^{\mu t} - f'(\theta)\phi_n(x)e^{\mu t}.
\end{aligned}$$

Eliminating $\phi_n(x)e^{\mu t}$ from both sides, we obtain the characteristic equation (2.7) when $m = 0$ for the weak kernel case. The calculation for the strong kernel case is similar. □

Theorem 2.4. *For Eq. (1.1) with the spatial kernel G taken as (1.4) and temporal kernel g as (1.7), the constant equilibrium $u = \theta$ is locally asymptotically stable (unstable) when the equilibrium of the equivalent system (2.2) or (2.4) is locally asymptotically stable (unstable).*

Proof. Here we still demonstrate the weak kernel case. From Lemma 2.3, the eigenvalues of the linear equation of Eq. (1.1) with weak kernel satisfy

$$\mu + d_1\lambda_n + \frac{d_2\theta\lambda_n}{1 + d_1\lambda_n\tau + \mu\tau} - f'(\theta) = 0. \tag{2.8}$$

By separating variable method for classical reaction-diffusion equations, it is eqsy to obtain the characteristic equation for its equivalent two-component system (2.1):

$$(\mu + d_1\lambda_n - f'(\theta))\left(\mu + d_1\lambda_n + \frac{1}{\tau}\right) + \frac{d_2\theta\lambda_n}{\tau} = 0. \tag{2.9}$$

A direct calculation shows that Eqs. (2.8) and (2.9) are completely equivalent to each other. A similar procedure can be applied to the strong kernel case and even Gamma functions with larger m. □

Remark 2.5. *1. Eq.* (1.1) *with the spatial kernel* G *taken as* (1.4) *and temporal kernel* g *as the general Gamma distribution function of order* n *in* (1.6) *is equivalent to a system of* $(n+1)$ *reaction-diffusion equations, and the system consists of one equation with chemotaxis and* n *linear equations.*

2. The equivalence of stability in Lemma 2.3 and Theorem 2.4 also hold for general Gamma distribution function of order n*, and the characteristic equation is* (2.7) *for* $m = n$*.*

3 Weak kernel case

From Theorem 2.4, the stability of the constant equilibrium $u = \theta$ with respect to (1.1) for the weak kernel case can be equivalently obtained through analyzing the following reaction-diffusion system with chemotaxis:

$$\begin{cases} u_t(x,t) = d_1\Delta u(x,t) + d_2 div(u(x,t)\nabla v(x,t)) + f(u(x,t)), & x \in \Omega,\ t > 0, \\ v_t(x,t) = d_1\Delta v(x,t) + \frac{1}{\tau}(u(x,t) - v(x,t)), & x \in \Omega,\ t > 0, \\ \partial_n u(x,t) = \partial_n v(x,t) = 0, & x \in \partial\Omega,\ t > 0, \end{cases} \tag{3.1}$$

which admits a constant equilibrium (θ, θ). Here we analyze the stability of (θ, θ) with respect to (3.1) and associated bifurcation of non-constant steady states. Similar stability analysis and bifurcation results have also been obtained in for example [20, 25]. We will provide detailed calculation for bifurcation direction and the stability of the bifurcating steady state.

First we linearize Eq. (2.1) at (θ, θ), and the stability of of (θ, θ) with respect to (3.1) is determined by eigenvalue problem

$$\begin{cases} d_1\Delta\varphi + d_2\theta\Delta\psi + f'(\theta)\varphi = \mu\varphi, & x \in \Omega, \\ d_1\Delta\psi + \frac{1}{\tau}(\varphi - \psi) = \mu\psi, & x \in \Omega, \\ \partial_n\varphi = \partial_n\psi = 0, & x \in \partial\Omega. \end{cases} \tag{3.2}$$

By using the results of Lemma 3.1 in [31], the eigenvalues of (3.2) are the eigenvalues of Jacobian matrix

$$J_n^w = \begin{pmatrix} -d_1\lambda_n + f'(\theta) & -d_2\theta\lambda_n \\ \frac{1}{\tau} & -d_1\lambda_n - \frac{1}{\tau} \end{pmatrix}, \tag{3.3}$$

where λ_n is the eigenvalues of (1.5) for $n \in \mathbb{N}_0$. Hence we have the characteristic equations:

$$\mu^2 + T_n\mu + D_n = 0, \quad n \in \mathbb{N}_0, \tag{3.4}$$

with

$$T_n = 2d_1\lambda_n + \frac{1}{\tau} - f'(\theta), \quad D_n = d_1^2\lambda_n^2 + \left(\frac{d_1 + d_2\theta}{\tau} - d_1 f'(\theta)\right)\lambda_n - \frac{f'(\theta)}{\tau}. \tag{3.5}$$

Note that $T_n = -Trace(J_n^w)$ and $D_n = Det(J_n^w)$.

From (H1) we have $f'(\theta) < 0$, hence $T_n > 0$ for all $n \in \mathbb{N}_0$ and the necessary for Hopf bifurcation $T_n = 0$ cannot be satisfied. For steady state bifurcations we have the following results for Eq. (3.4).

Lemma 3.1. *Define*

$$d_{2,n}^w = \frac{(f'(\theta) - d_1\lambda_n)(d_1\lambda_n\tau + 1)}{\theta\lambda_n},\ d_2^* = \max_{n\in\mathbb{N}} d_{2,n}^w \tag{3.6}$$

Then, the following results hold:

(i) *Eq.* (3.4) *has no purely imaginary roots for any* $d_2 \in \mathbb{R}$*;*

(ii) $\mu = 0$ *is a root of Eq.* (3.4) *if and only if* $d_2 = d_{2,n}^w$*;*

(iii) *when* $d_2 > d_2^*$*, all the eigenvalues of Eq.* (3.4) *have negative real parts; when* $d_2 < d_2^*$*,* (3.4) *has at least one eigenvalue with positive real part.*

Proof. Conclusion (i) can be easily seen as $T_n > 0$ for all $n \in \mathbb{N} \cup \{0\}$ and any $d_2 \in \mathbb{R}$, while $T_n = 0$ is the necessary condition for Eq. (3.4) to have purely imaginary roots. Taking d_2 as the bifurcation parameter, we immediately obtain the steady state bifurcation points $d_2 = d_{2,n}^w$ satisfying $D_n(d_{2,n}^w) = 0$ such that Eq. (3.4) has a zero eigenvalue. This proves (ii). (iii) is a direct corollary of the definition of d_2^*. □

Based on Lemma 3.1, we obtain the following results for the stability of (θ, θ) of Eq. (3.1).

Theorem 3.2. *Suppose that* $d_1,\ d_2,\ f$ *satisfy (H1) and (H2), and let* d_2^* *be defined in Lemma 3.1. Then,* (θ, θ) *is locally asymptotically stable if* $d_2 \geq d_2^*$ *and it is unstable if* $d_2 < d_2^*$*.*

Next we show the bifurcation of non-constant steady state solution following [6, 29, 32]. A steady state of Eq. (3.1) is a solution of the elliptic system:

$$\begin{cases} d_1\Delta u + d_2 div(u\nabla v) + f(u) = 0, & x \in \Omega, \\ d_1\Delta v + \frac{1}{\tau}(u - v) = 0, & x \in \Omega, \\ \partial_n u = \partial_n v = 0, & x \in \partial\Omega. \end{cases} \tag{3.7}$$

In the following, we prove the occurrence of steady state bifurcations in system (3.7).

Theorem 3.3. *Suppose that* $d_1,\ d_2$ *and* f *satisfy (H1) and (H2), and let* d_2^**,* $d_{2,n}^w$ *be defined in Lemma 3.1.*

(i) *Suppose that* λ_n *is a simple eigenvalue of* (1.5)*, and* $d_{2,n}^w \neq d_{2,k}^w$ *for any* $k \in \mathbb{N}$ *and* $k \neq n$*. Then* $d_2 = d_{2,n}^w$ *is a bifurcation point for* (3.7)*. More precisely, near* $(d_{2,n}^w, \theta, \theta)$*, there is a smooth curve* Γ_n *of positive solutions of* (3.7) *bifurcating from the line of constant solutions* $\{(d_2, \theta, \theta) : d_2 > 0\}$ *with the following form:*

$$\Gamma_n = \{(d_{2,n}(s), U_n(s,x), V_n(s,x)) : -\delta < s < \delta\}, \tag{3.8}$$

where δ *is a positive constant and*

$$U_n(s,x) = \theta + s\phi_n(x) + sz_{1,n}(s,x),\ V_n(s,x) = \theta + s\frac{\phi_n(x)}{d_1\lambda_n\tau + 1} + sz_{2,n}(s,x),$$

with smooth functions $d_{2,n}(s),\ z_{1,n}(s,\cdot),\ z_{2,n}(s,\cdot)$ *satisfying* $d_{2,n}(0) = d_{2,n}^w$ *and* $z_{1,n}(0,\cdot) = 0,\ z_{2,n}(0,\cdot) = 0$*;*

(ii) *If in addition,* Ω *is one-dimensional and* $\Omega = (0, l\pi)$*, then* $d_{2,n}'(0) = 0$ *and*

$$d_{2,n}''(0) = \frac{f'''(\theta)}{4\theta\lambda_n h_n} + \frac{2(f''(\theta) - d_{2,n}^w\lambda_n h_n)\Theta_1^0) + f''(\theta)\Theta_1^2 - 2d_{2,n}^w\lambda_n\Theta_2^2 + d_{2,n}^w\lambda_n h_n\Theta_1^2}{2\theta\lambda_n h_n}, \tag{3.9}$$

where $\Theta_1^0,\ \Theta_1^2,\ \Theta_2^2$ *are given by*

$$\begin{aligned} \Theta_1^0 &= -\frac{f''(\theta)}{2f'(\theta)},\ \Theta_1^2 = \frac{(4d_{2,n}^w\lambda_n h_n - f''(\theta))(1 + 4d_1\lambda_n\tau)}{2[(f'(\theta) - 4d_1\lambda_n)(1 + 4d_1\tau\lambda_n)^2 - 4d_{2,n}^w\theta\lambda_n]}, \\ \Theta_2^2 &= \frac{4d_{2,n}^w\lambda_n h_n - f''(\theta)}{2[(f'(\theta) - 4d_1\lambda_n)(1 + 4d_1\tau\lambda_n)^2 - 4d_{2,n}^w\theta\lambda_n]}, \end{aligned} \tag{3.10}$$

and $\lambda_n = n^2/l^2,\ h_n = 1/(1 + d_1\lambda_n\tau)$*. Let* $d_{2,N}^w = d_2^*$*. If* $d_{2,N}''(0) < 0$*, the bifurcation at* $d_2 = d_2^* = d_{2,N}^w$ *is supercritical and the bifurcating steady states are locally asymptotically stable; if* $d_{2,N}''(0) > 0$*, the bifurcation at* $d_2 = d_2^* = d_{2,N}^w$ *is subcritical and the bifurcating steady states are unstable; all other bifurcating steady states from* $d_{2,n}^w$ *with* $n \neq N$ *are unstable.*

The proof of Theorem 3.3 is given in the Appendix. From Theorems 3.2 and 3.3, $d_2 = d_2^* < 0$ is a critical diffusion rate where the constant steady state (θ, θ) changes stability, and it is rigorously shown that small amplitude stable non-homogeneous steady state solutions could bifurcate from the constant ones at $d_2 = d_2^*$.

Remark 3.4. *1. Theorem 3.3 is a local bifurcation result as the nonlinear function* f *is only defined in a neighborhood of* $u = \theta$*. One may obtain a global bifurcation diagram by using the abstract bifurcation theorem in [32] for a globally defined nonlinearity* $f(u)$*, but this is not pursued here.*

2. *In the discrete delay model considered in [31], a necessary condition for pattern formation is that $|d_2| > d_1/\theta$. In the case of (1.1) with weak kernel, a necessary condition for pattern formation is $d_2 < d_2^* \leq -(\sqrt{-\tau f'(\theta)}+1)^2 d_1/\theta$ which implies that $d_2 < -d_1/\theta$. Thus, we see that $|d_2| > d_1/\theta$ is still necessary for the pattern formation in the distributed delay case, but the delay value τ increases the threshold $|d_2^*| = |d_2^*(\tau)|$. So to achieve pattern formation, the magnitude of the memory-based diffusion needs to be larger in the distributed delay case than in the discrete delay case.*

3. *The average delay value τ also affects the pattern selection. Let N be the dominant wave number which satisfies $d_{2,N}^w = d_2^*$ as in Theorem 3.3. Then N is non-increasing with respect to τ. Indeed one can observe that when we consider $d_{2,n}^w$ as a function of continuous variable $p = \lambda_n$ in (3.6), it reaches it maximum at $p = \sqrt{\frac{-f'(\theta)}{\tau d_1^2}}$. Hence*

$$\lambda_N = \frac{N^2}{l^2} \approx \sqrt{\frac{-f'(\theta)}{\tau d_1^2}}, \tag{3.11}$$

which implies that N is non-increasing with respect to τ.

4 Strong kernel case

From Theorem 2.4, the stability of the constant equilibrium $u = \theta$ with respect to (1.1) for the strong kernel case can be equivalently obtained through analyzing the following reaction-diffusion system with chemotaxis:

$$\begin{cases} u_t(x,t) = d_1\Delta u(x,t) + d_2 div(u(x,t)\nabla v(x,t)) + f(u(x,t)), & x \in \Omega,\ t > 0, \\ v_t(x,t) = d_1\Delta v(x,t) + \frac{1}{\tau}(w(x,t) - v(x,t)), & x \in \Omega,\ t > 0, \\ w_t(x,t) = d_1\Delta w(x,t) + \frac{1}{\tau}(u(x,t) - w(x,t)), & x \in \Omega,\ t > 0, \\ \partial_n u(x,t) = \partial_n v(x,t) = \partial_n w(x,t) = 0, & x \in \partial\Omega,\ t > 0, \end{cases} \tag{4.1}$$

which admits a constant equilibrium (θ, θ, θ). Linearizing Eq. (4.1) at (θ, θ), and the stability of of (θ, θ, θ) with respect to (4.1) is determined by eigenvalue problem:

$$\begin{cases} d_1\Delta\phi + d_2\theta\Delta\psi + f'(\theta)\phi = \mu\phi, & x \in \Omega, \\ d_1\Delta\psi + \frac{1}{\tau}(\varphi - \psi) = \mu\psi, & x \in \Omega, \\ d_1\Delta\varphi + \frac{1}{\tau}(\phi - \varphi), & x \in \Omega, \\ \partial_n\phi = \partial_n\psi = \partial_n\varphi, & x \in \partial\Omega. \end{cases} \tag{4.2}$$

Similar to the weak kernel case, the eigenvalues of (4.2) are the eigenvalues of Jacobian matrix

$$J_n^s = \begin{pmatrix} -d_1\lambda_n + f'(\theta) & -d_2\theta\lambda_n & 0 \\ 0 & -d_1\lambda_n - \frac{1}{\tau} & \frac{1}{\tau} \\ \frac{1}{\tau} & 0 & -d_1\lambda_n - \frac{1}{\tau} \end{pmatrix},$$

where λ_n is the eigenvalues of (1.5) for $n \in \mathbb{N}_0$. Hence we have the characteristic equations:

$$\mu^3 + A_n\mu^2 + B_n\mu + C_n = 0, \ \ n \in \mathbb{N}_0, \tag{4.3}$$

with

$$\begin{aligned} A_n &= 3d_1\lambda_n + \frac{2}{\tau} - f'(\theta), \\ B_n &= \left(d_1\lambda_n + \frac{1}{\tau}\right)^2 + 2(d_1\lambda_n - f'(\theta))\left(d_1\lambda_n + \frac{1}{\tau}\right), \\ C_n &= d_1^3\lambda_n^3 + \left(\frac{2d_1^2}{\tau} - f'(\theta)d_1^2\right)\lambda_n^2 + \left(\frac{d_1 + d_2\theta}{\tau} - \frac{2f'(\theta)d_1}{\tau}\right)\lambda_n - \frac{f'(\theta)}{\tau^2}. \end{aligned} \tag{4.4}$$

Note that $A_n = -Trace(J_n^s)$ and $C_n = -Det(J_n^s)$. By the Routh-Hurwitz stability criterion, the matrix J_n^s is stable (all eigenvalues have negative real part) if and only if

$$A_n > 0, \ \ C_n > 0, \ \ A_nB_n - C_n > 0.$$

From (H1), the condition $A_n > 0$ always holds. Hence the matrix J_n^s may lose the stability either via $C_n = 0$ (which implies a zero eigenvalue of J_n^s) or via $A_nB_n - C_n = 0$ (which implies a pair of purely imaginary eigenvalues of J_n^s).

To study these two kinds of instability, we define continuous functions $A(p), B(p), C(p)$ for $p \in [0, \infty)$ so that $A(\lambda_n) = A_n$, $B(\lambda_n) = B_n$ and $C(\lambda_n) = C_n$. Then

$$\begin{aligned} C(p) &:= d_1^3p^3 + a_1p^2 + b_1p + c_1, \\ Q(p) &:= A(p)B(p) - C(p) = 8d_1^3p^3 + a_2p^2 + b_2p + c_2, \end{aligned} \tag{4.5}$$

where

$$\begin{aligned} &a_1 = \frac{2d_1^2}{\tau} - f'(\theta)d_1^2, \ b_1 = \frac{d_1 + d_2\theta}{\tau^2} - \frac{2f'(\theta)d_1}{\tau}, \ c_1 = -\frac{f'(\theta)}{\tau^2}, \\ &a_2 = \frac{16d_1^2}{\tau} - 8f'(\theta)d_1^2, \ b_2 = \frac{10d_1 - d_2\theta}{\tau^2} - \frac{12d_1f'(\theta)}{\tau} + 2d_1(f'(\theta))^2, \ c_2 = \frac{2}{\tau}\left(\frac{1}{\tau} - f'(\theta)\right)^2. \end{aligned}$$

Taking d_2 as the parameter, we obtain the steady state bifurcation points:

$$d_{2,n}^S := d_2^S(\lambda_n), \ \text{with } d_2^S(p) = \frac{(f'(\theta) - d_1p)(d_1p\tau + 1)^2}{\theta p}, \tag{4.6}$$

and Hopf bifurcation points:

$$d_{2,n}^H := d_2^H(\lambda_n), \ \text{with } d_2^H(p) = \frac{2(d_1\tau p + 1)(2d_1\tau p - f'(\theta)\tau + 1)^2}{\theta\tau p}. \tag{4.7}$$

Note that $d_2 = d_2^S(p)$ is solved from setting $C(p) = 0$, so $d_{2,n}^S$ satisfies $C(\lambda_n) = 0$. Similarly $d_2 = d_{2,n}^H$ is solved from setting $Q(p) = 0$, so $d_{2,n}^H$ satisfies $Q(\lambda_n) = 0$.

Some basic properties of functions $d_2^S(p)$ and $d_2^H(p)$ are stated in the following lemma.

Lemma 4.1. *For $d_2^S(p)$ and $d_2^H(p)$ defined in (4.6) and (4.7), we have*

(i) *there exists $p_* > 0$ such that $d_2^S(p)$ is increasing for $p \in (0, p_*)$ and decreasing for $p \in (p_*, +\infty)$, and $d_2^S(p)$ attains its global maximum value $d_{2,S}^* < 0$ at $p = p_*$. Moreover, we have $\lim_{p\to 0} d_2^S(p) = -\infty$ and $\lim_{p\to+\infty} d_2^S(p) = -\infty$.*

(ii) *there exists $p^* > 0$ such that d_2^H is decreasing for $p \in (0, p^*)$ and increasing for $p \in (p^*, +\infty)$, and $d_2^H(p)$ attains its global minimum value $d_{2,H}^* > 0$ at $p = p^*$. Moreover, we have $\lim_{p\to 0} d_2^H(p) = +\infty$ and $\lim_{p\to+\infty} d_2^H(p) = +\infty$.*

Proof. With the expression of $d_2^S(p)$ given in (4.6), we calculate the derivative of $d_2^S(p)$ with respect to p and obtain

$$\frac{d}{dp} d_2^S(p) = \frac{(d_1 p\tau + 1)H(p)}{\theta^2 p^2}, \tag{4.8}$$

with

$$H(p) = -2d_1^2\tau\theta p^2 + d_1\tau\theta f'(\theta)p - f'(\theta)\theta.$$

From Eq. (4.8), we can see that the sign of the derivative of $d_2^S(p)$ is the same as the one of $H(p)$ which is a quadric function with a unique positive root p_*. Thus, we have $H(p) > 0$ for $p \in (0, p_*)$ and $H(p) < 0$ for $p \in (p_*, +\infty)$. The limits of d_2^S when $p \to 0$ and $p \to +\infty$ can be attained through a direct calculation. This proves part (i). Part (ii) can be proved in a similar way. □

We obtain the stability of (θ, θ, θ) for Eq. (4.1) as follows.

Proposition 4.2. *Suppose that d_1, d_2, f satisfy conditions (H1) and (H2) and $\tau > 0$. Define*

$$d_{2,S}^* := \max_{n\in\mathbb{N}} \left\{ d_{2,n}^S \right\}, \ d_{2,H}^* := \min_{n\in\mathbb{N}} \left\{ d_{2,n}^H \right\}, \tag{4.9}$$

where $d_{2,n}^S$ and $d_{2,n}^H$ are defined in (4.6) and (4.7).

(i) *when $d_{2,S}^* < d_2 < d_{2,H}^*$, all the eigenvalues of Eq. (4.3) have negative real parts, and (θ, θ, θ) is locally asymptotically stable with respect to (4.1);*

(ii) *when $d_2 > d_{2,H}^*$, (θ, θ, θ) is unstable and $\mu = \pm i\omega_0$ $(\omega_0 > 0)$ is a pair of purely imaginary roots of Eq. (4.3) if $d_2 = d_{2,n}^H$;*

(iii) *when $d_2 < d_{2,S}^*$, (θ, θ, θ) is unstable and $\mu = 0$ is a root of Eq. (4.3) if $d_2 = d_{2,n}^S$.*

Proof. From Lemma 4.1, when $d_{2,S}^* < d_2 < d_{2,H}^*$, we have $C(p) > 0$ and $Q(p) > 0$ for all $p > 0$ so all the eigenvalues of J_n^s have negative real parts for $n \in \mathbb{N}_0$ thus (θ, θ, θ) is locally asymptotically stable. When $d_2 < d_{2,n}^S$, we have $C_n < 0$ so the matrix J_n^s has at least one eigenvalue with positive real part, and when $d_2 = d_{2,n}^S$, J_n^s has a zero eigenvalue. This implies (θ, θ, θ) when $d_2 < d_{2,S}^*$. When $d_2 > d_{2,n}^H$, we have $A_n > 0$, $C_n > 0$ but $A_n B_n - C_n < 0$, so the matrix J_n^s is unstable, and when $d_2 = d_{2,n}^H$, J_n^s has a pair of complex eigenvalues with zero real part. □

From Proposition 4.2, Eq. (4.3) has a pair of purely imaginary eigenvalues $\pm i\omega_0$ ($\omega_0 > 0$) when $d_2 = d_{2,n}^H$. We show that the eigenvalue transversality condition holds at $d_2 = d_{2,n}^H$.

Lemma 4.3. *Let $d_{2,n}^H$ be defined in* (4.7)*. Then, Eq.* (4.3) *has a pair of roots in the form of $\mu = \alpha(d_2) \pm i\omega(d_2)$ when d_2 is near $d_{2,n}^H$ such that $\alpha\left(d_{2,n}^H\right) = 0$ and $\alpha'\left(d_{2,n}^H\right) > 0$.*

Proof. We only need to show that $\alpha'\left(d_{2,n}^H\right) < 0$. Take derivative of both sides of Eq. (4.3) with respect to d_2 (we denote d_2 temporarily by β to avoid the confusion in notation), we have

$$3\mu^2 \frac{d\mu}{d\beta} + \frac{dA_n}{d\beta}\mu^2 + 2A_n\mu\frac{d\mu}{d\beta} + \frac{dB_n}{d\beta}\mu + B_n\frac{d\mu}{d\beta} + \frac{dC_n}{d\beta} = 0. \tag{4.10}$$

From the expressions of $A_n,\ B_n,\ C_n$ in Eq. (4.3), it is straightforward to see that

$$\frac{dA_n}{d\beta} = 0,\ \frac{dB_n}{d\beta} = 0,\ \frac{dC_n}{d\beta} = \frac{\theta\lambda_n}{\tau}. \tag{4.11}$$

Substituting (4.11), $\mu = i\omega_0$, $B_n = \omega_0^2$ and $\beta = d_{2,n}^H$ into Eq. (4.10), we obtain

$$\frac{d\mu}{d\beta}\Big|_{\beta = d_{2,n}^H} = -\frac{\theta\lambda_n}{2\tau\omega_0(-\omega_0^2 + i\omega_0 A_n)},$$

thus

$$\alpha'(d_2) = \mathcal{R}e\left(\frac{d\mu}{d\beta}\Big|_{\beta = d_{2,n}^H}\right) = \frac{\theta\lambda_n}{2\tau(\omega_0^2 + A_n^2)} > 0.$$

□

Now by the Hopf bifurcation Theorem for quasilinear systems of reaction-diffusion equations [2], Proposition 4.2 and Lemma 4.3, we obtain the following result of Hopf bifurcations in Eq. (4.1).

Theorem 4.4. *Suppose that d_1, d_2, and f satisfy conditions (H1) and (H2), and let $d_{2,n}^H$ be defined in* (4.7)*. Suppose that λ_n is a simple eigenvalue of* (1.5)*, and $d_{2,n}^H \neq d_{2,k}^H$ for any $k \in \mathbb{N}$ and $k \neq n$, then a Hopf bifurcation occurs at $d_2 = d_{2,n}^H$ for Eq.* (4.1) *and there exist a family of periodic orbits in form of*

$$\left\{\left(U_n(x,t,s), T_n(s), d_2^{(n)}(s)\right) : s \in (0,\delta)\right\},$$

where $U_n(x,t,s)=(u_n(x,t,s),v_n(x,t,s),w_n(x,t,s))$ *is a* $T_n(s)$ *periodic solution of Eq.* (4.1) *with* $d_2=d_2^{(n)}(s)$ *satisfying*

$$d_2^{(n)}(0)=d_{2,n}^H,\ \lim_{s\to 0}U_n(x,t,s)=(\theta,\theta,\theta),\ \lim_{s\to 0}T_n(s)=\frac{2\pi}{\sqrt{B_n}},$$

where B_n *is given in* (4.4). *Moreover, the bifurcating periodic orbits are spatially non-homogeneous with spatial profile* $\phi_n(x)$.

At $d_2=d_{2,H}^*=\min_{n\in\mathbb{N}}d_{2,n}^H$, the bifurcating periodic orbits could be locally asymptotically stable, and if $d_{2,M}^H=d_{2,H}^*$ for some $M\in\mathbb{N}$, then the stable bifurcating periodic orbits have the spatial profile $\phi_M(x)$ and are temporally oscillating with period $T_M(s)$.

We can also prove the steady state bifurcations for (4.1) at $d_2=d_{2,n}^S$ similar to the weak kernel case. The steady states of (4.1) satisfy the following elliptic system:

$$\begin{cases} d_1\Delta u(x)+d_2 div(u(x)\nabla v(x))+f(u(x))=0, & x\in\Omega,\\ d_1\Delta v(x)+\frac{1}{\tau}(w(x)-v(x))=0, & x\in\Omega,\\ d_1\Delta w(x)+\frac{1}{\tau}(u(x)-w(x))=0, & x\in\Omega,\\ \partial_n u(x)=\partial_n v(x)=\partial_n w(x)=0, & x\in\partial\Omega, \end{cases} \tag{4.12}$$

and (θ,θ,θ) is a constant solution for system (4.12). Then we have the following results.

Theorem 4.5. *Suppose that* d_1, d_2, *and* f *satisfy conditions (H1) and (H2), and let* $d_{2,n}^S$ *be defined in* (4.6).

(i) *Suppose that* λ_n *is a simple eigenvalue of* (1.5), *and* $d_{2,n}^S\neq d_{2,k}^S$ *for any* $k\in\mathbb{N}$ *and* $k\neq n$. *Then* $d_2=d_{2,n}^S$ *is a bifurcation point for* (4.12). *More precisely, near* $(d_{2,n}^S,\theta,\theta,\theta)$, *there is a smooth curve* $\tilde{\Gamma}_n$ *of positive solutions of* (4.12) *bifurcating from the line of constant solutions* $\{(d_2,\theta,\theta,\theta):d_2>0\}$ *with the following form:*

$$\tilde{\Gamma}_n=\left\{\left(\tilde{d}_{2,n}(s),U^n(s,x),V^n(s,x),W^n(s,x)\right):\ -\delta<s<\delta\right\}, \tag{4.13}$$

where

$$\begin{aligned} U^n(s,x)&=\theta+s\phi_n(x)+sg_{1,n}(s,x),\\ V^n(s,x)&=\theta+\frac{1}{(1+d_1\lambda_n\tau)^2}s\phi_n(x)+sg_{2,n}(s,x),\\ W^n(s,x)&=\theta+\frac{1}{1+d_1\lambda_n\tau}s\phi_n(x)+sg_{3,n}(s,x), \end{aligned}$$

and $\tilde{d}_{2,n}(s)$, $g_{i,n}(s,\cdot)(i=1,2,3)$ *are smooth functions defined for* $s\in(0,\delta)$ *such that* $\tilde{d}_{2,n}(0)=d_{2,n}^S$, *and* $g_{i,n}(0,\cdot)=0$ $(i=1,2,3)$;

(ii) *If in addition, Ω is one-dimensional and $\Omega = (0, l\pi)$, then $\tilde{d}'_{2,n}(0) = 0$ and*

$$\tilde{d}''_{2,n}(0) = \frac{f'''(\theta)}{4\lambda_n h_n \theta} + \frac{2(f''(\theta) - d^S_{2,n}\lambda_n h_n)\Theta^0_1) + f''(\theta)\Theta^2_1 - 2d^S_{2,n}\lambda_n\Theta^2_2 + d^S_{2,n}\lambda_n h_n \Theta^2_1}{2\theta\lambda_n h_n}, \tag{4.14}$$

where $\Theta^0_1,\ \Theta^2_1,\ \Theta^2_2$ are given by

$$\begin{aligned} \Theta^0_1 &= -\frac{f''(\theta)}{2f'(\theta)},\ \Theta^2_1 = \frac{(4d^S_{2,n}\lambda_n h_n - f''(\theta))(1 + 4d_1\lambda_n\tau)}{2[(f'(\theta) - 4d_1\lambda_n)(1 + 4d_1\tau\lambda_n)^2 - 4d^S_{2,n}\theta\lambda_n]}, \\ \Theta^2_2 &= \frac{4d^S_{2,n}\lambda_n h_n - f''(\theta)}{2[(f'(\theta) - 4d_1\lambda_n)(1 + 4d_1\tau\lambda_n)^2 - 4d^S_{2,n}\theta\lambda_n]}, \end{aligned} \tag{4.15}$$

and $\lambda_n = n^2/l^2$, $h_n = 1/(1 + d_1\lambda_n\tau)^2$. Let $d^S_{2,N} = d^*_{2,S}$. If $\tilde{d}''_{2,N}(0) < 0$, the bifurcation at $d_2 = d^*_{2,S} = d^S_{2,N}$ is supercritical and the bifurcating steady states are locally asymptotically stable; if $\tilde{d}''_{2,N}(0) > 0$, the bifurcation at $d_2 = d^*_{2,S} = d^S_{2,N}$ is subcritical and the bifurcating steady states are unstable; all other bifurcating steady states from $d^S_{2,n}$ with $n \neq N$ are unstable.

The proof of Theorem 4.5 is basically the same as the one for Theorem 3.3, so we omit the proof.

Remark 4.6. *1. From Lemma 4.1, it is clear that all steady state bifurcation points $d^S_{2,n} < 0$ and all Hopf bifurcation points $d^H_{2,n} > 0$ for $n \in \mathbb{N}$, which implies that there is no interaction between steady state bifurcations and Hopf bifurcations in this model. Steady state bifurcations only occur for negative d_2 (attractive chemotaxis case), and Hopf bifurcations only occur for positive d_2 (repulsive chemotaxis case).*

2. From (4.6), we can obtain that $d^S_{2,n} < -d_1/\theta$, thus $d^*_{2,S} < -d_1/\theta$. Similarly, we have $d^*_{2,H} > 2d_1/\theta$. Therefore, we can draw the conclusion that $|d_2| > d_1/\theta$ is still a necessary condition for pattern formation in the distributed delay case with strong kernel.

3. Again the average delay value τ affects the pattern selection for both steady state and Hopf bifurcations. If positive integer N and M satisfy $d^S_{2,N} = d^*_{2,S}$ and $d^H_{2,M} = d^*_{2,H}$, then N and M both are non-increasing with respect to τ.

5 An example: Logistic growth

When the growth function $f(u)$ is taken as the logistic growth, Eq. (1.1) becomes

$$\begin{cases} u_t = d_1\Delta u + d_2 div(u\nabla v) + u(1-u), & x \in \Omega,\ t > 0, \\ \partial_n u = 0, & x \in \partial\Omega,\ t > 0, \end{cases} \tag{5.1}$$

where $u = u(x,t)$ and $v = v(x,t)$ is defined as (1.2). It is clear that Eq (5.1) has two constant equilibria: $u = 0$ and $u = 1$.

5.1 Weak kernel case

For the weak kernel case, (5.1) is equivalent to

$$\begin{cases} u_t = d_1\Delta u + d_2 div(u\nabla v) + u(1-u), & x \in \Omega,\ t > 0, \\ v_t = d_1\Delta v + \frac{1}{\tau}(u-v), & x \in \Omega,\ t > 0, \\ \partial_n u = \partial_n v = 0, & x \in \partial\Omega,\ t > 0. \end{cases} \tag{5.2}$$

Apparently, the trivial equilibrium $(0,0)$ is unstable. We can apply Theorems 3.2 and 3.3 for the stability of the positive equilibrium $(1,1)$ and the bifurcation of non-homogeneous steady states of system (5.2) as $f'(\theta) = -1$ so (H1) is satisfied. The bifurcation points are

$$d_2 = d_{2,n}^w = -\frac{(1+d_1\lambda_n)(1+d_1\lambda_n\tau)}{\theta\lambda_n}, \tag{5.3}$$

and for one-dimensional domain $\Omega = (0, l\pi)$, we have

$$d''_{2,n}(0) = \frac{(1+d_1\lambda_n\tau)(5-2d_1^2\lambda_n^2\tau-5d_1\lambda_n+28d_1^3\lambda_n^3\tau+10d_1\lambda_n\tau-2d_1^2\lambda_n^2)}{6\lambda_n(1-4d_1^2\lambda_n^2\tau)}.$$

At the dominant wave number N so that $d_{2,S}^* = d_{2,N}^S$, we have the approximating formula (3.11) which now becomes $d_1\lambda_N = 1/\sqrt{\tau}$. Using this yields

$$d''_{2,n}(0) = -\frac{d_1\sqrt{\tau}(1+\sqrt{\tau})\left(10\sqrt{\tau}+\frac{23}{\sqrt{\tau}}-\frac{2}{\tau}+3\right)}{18} < 0,$$

for any $\tau > 0$. This implies that the bifurcation direction of steady state bifurcation at the dominant wave number is most likely to be supercritical and the bifurcating steady states are locally asymptotically stable.

Fig. 1 shows the bifurcation diagram of system (5.2) in parameters d_2 and τ, where $d_1 = 0.1$ and $\Omega = (0,\pi)$. For a fixed τ, when d_2 varies from right to left, the constant equilibrium $(1,1)$ loses its stability at the first Turing bifurcation curve $d_2 = d_{2,n}^w(\tau)$ as defined in (5.3). One can observe that when τ decreases, the dominant wave number N changes from $N = 2$ to $N = 3$ then $N = 4$. When $\tau = 4$, the stability switch occurs at mode-2 Turing line, and the constant equilibrium is stable when $d_2 = -0.86$ (P1) and unstable when $d_2 = -0.93$ (P2) (Fig. 2 top row); when $\tau = 1.5$, the stability switch occurs at mode-3, and the constant equilibrium is stable when $d_2 = -0.45$ (P3) and unstable when $d_2 = -0.52$ (P4) (Fig. 2 middle row). In the stable case, the solution converges to the constant equilibrium, while in the unstable case, the solution converges to a mode-N non-homogeneous steady

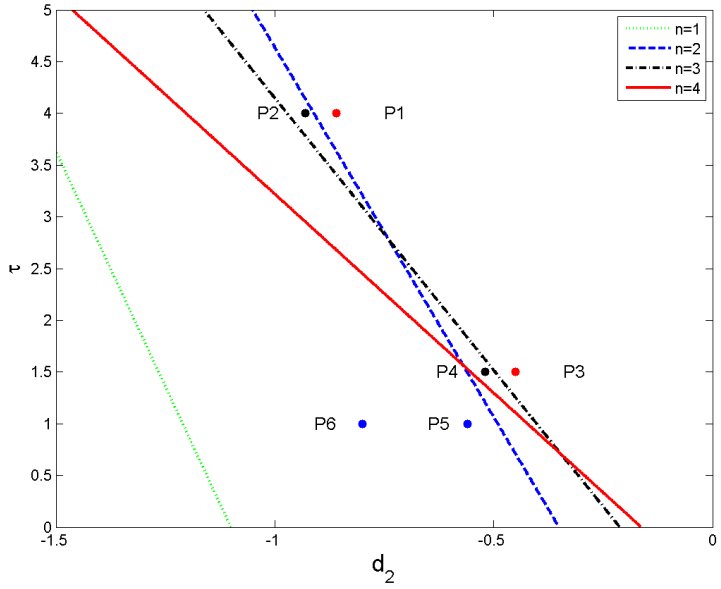

Figure 1: The bifurcation diagram in parameter (d_2, τ) of system (5.2) when $d_1 = 0.1$ and $\Omega = (0, \pi)$, and the bifurcation curves $d_2 = d_{2,n}^w(\tau)$ are plotted for $n = 1, 2, 3, 4$. The points are parameter values for the numerical simulations and they are: P1 $(-0.86, 4.0)$, P2 $(-0.93, 4.0)$, P3 $(-0.45, 1.5)$, P4 $(-0.52, 1.5)$, P5 $(-0.56, 1.0)$ and P6 $(-0.8, 1.0)$.

state. When d_2 is chosen as smaller values, we also observe spatially non-homogeneous time-periodic patterns shown in Fig. 2 bottom row, which are "wandering" and "drifting" periodic patterns also observed in previous work of Keller-Segel model with growth [20, 25]. These patterns are not a result of Hopf bifurcations from the constant equilibrium as we show that is impossible in Section 3.

5.2 Strong kernel case

When the distribution kernel is taken as the strong one, the equivalent system of Eq. (5.1) is

$$\begin{cases} u_t = d_1 \Delta u + d_2 div(u \nabla v) + u(1-u), & x \in \Omega,\ t > 0, \\ v_t = d_1 \Delta v + \frac{1}{\tau}(w - v), & x \in \Omega,\ t > 0, \\ w_t = d_1 \Delta w + \frac{1}{\tau}(u - w), & x \in \Omega,\ t > 0, \\ \partial_n u = \partial_n v = \partial_n w = 0, & x \in \partial\Omega,\ t > 0. \end{cases} \tag{5.4}$$

The trivial equilibrium $(0, 0, 0)$ is unstable, we can apply Theorems 4.5 and 4.4 for the stability of the positive equilibrium $(1, 1, 1)$ and the bifurcation of non-homogeneous steady states and

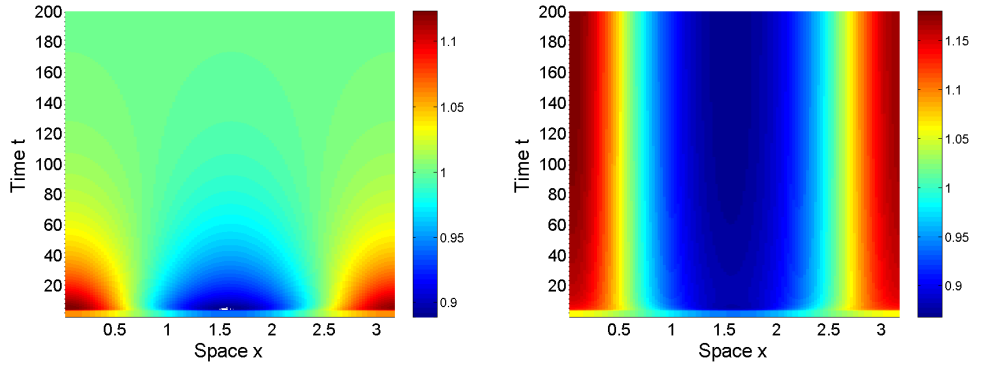

(a) $(d_1, \tau) = P1$ (b) $(d_1, \tau) = P2$

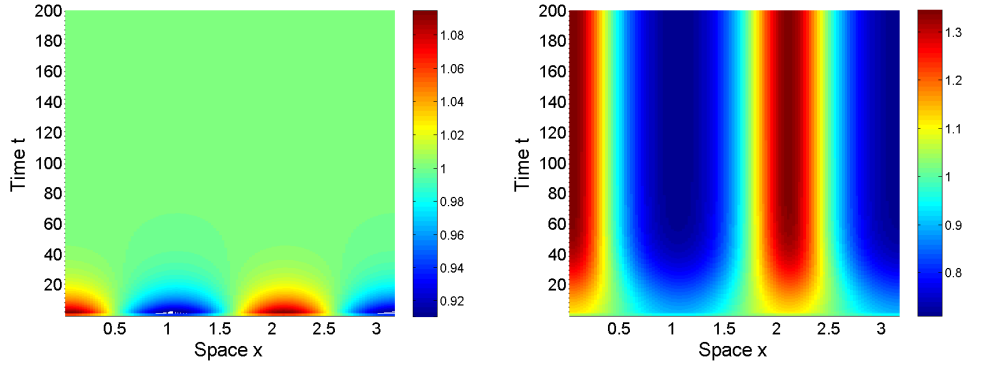

(c) $(d_1, \tau) = P3$ (d) $(d_1, \tau) = P4$

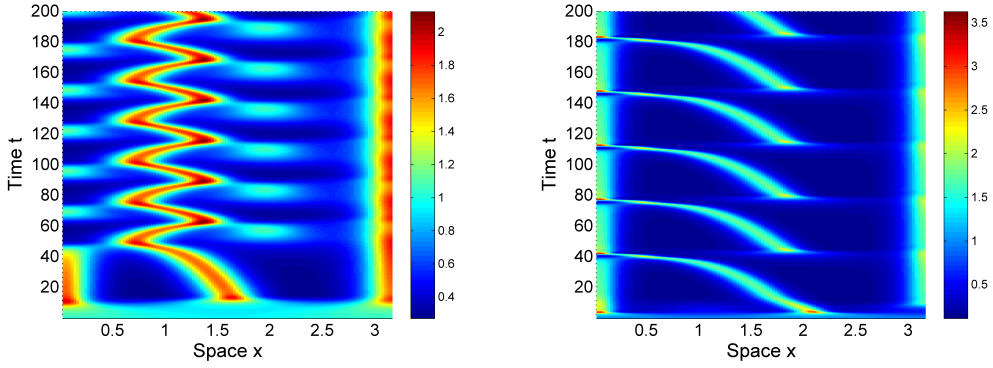

(e) $(d_1, \tau) = P5$ (f) $(d_1, \tau) = P6$

Figure 2: Numerical simulations of system (5.2) when parameters are $d_1 = 0.1$ and $\Omega = (0, \pi)$.

periodic orbits of system (5.4). The steady state bifurcations occur at

$$d_2 = d_{2,n}^S := -\frac{(1+d_1\lambda_n)(1+d_1\lambda_n\tau)^2}{\theta\lambda_n} < 0, \tag{5.5}$$

and the Hopf bifurcations occur at

$$d_2 = d_{2,n}^H = \frac{2(d_1\tau\lambda_n+1)(2d_1\tau\lambda_n+\tau+1)^2}{\theta\tau\lambda_n} > 0. \tag{5.6}$$

Fig. 3 shows the bifurcation diagram of system (5.4) in parameters d_2 and τ, where $d_1 = 0.1$ and $\Omega = (0,\pi)$. For a fixed τ, when d_2 varies from right to left starting from $d_2 = 0$, the constant equilibrium $(1,1,1)$ loses its stability at the first Turing bifurcation curve $d_2 = d_{2,n}^S(\tau)$ as defined in (5.5) to generate a spatial pattern; and similarly when d_2 varies from left to right starting from $d_2 = 0$, the constant equilibrium $(1,1,1)$ loses its stability at the first Hopf bifurcation curve $d_2 = d_{2,n}^H(\tau)$ as defined in (5.6) to generate a spatiotemporal pattern.

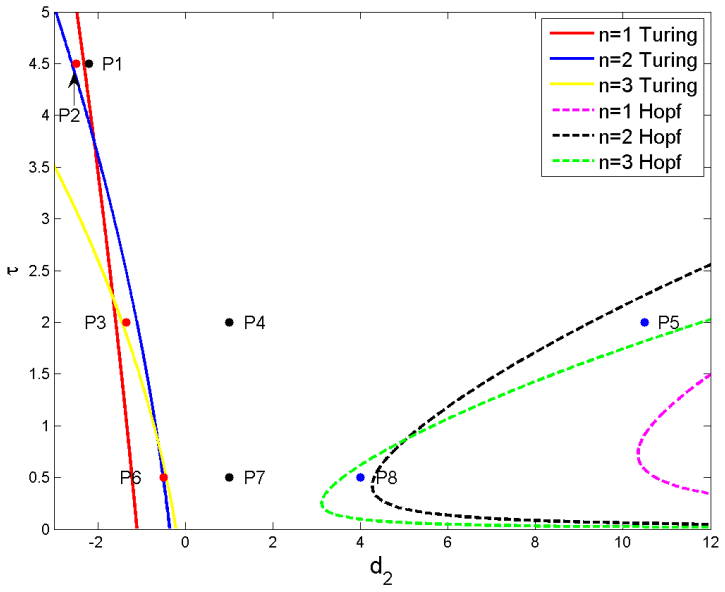

Figure 3: The bifurcation diagram in parameter (d_2,τ) of system (5.4) when $d_1 = 0.1$ and $\Omega = (0,\pi)$, and the steady state bifurcation curves $d_2 = d_{2,n}^S(\tau)$ (for $d_2 < 0$) and Hopf bifurcation curves $d_2 = d_{2,n}^H(\tau)$ (for $d_2 > 0$) are plotted for $n = 1,2,3$. The points are parameter values for the numerical simulations and they are: P1 $(-2.5, 4.5)$, P2 $(-2.2, 4.5)$, P3 $(-1.35, 2.0)$, P4 $(1.0, 2.0)$, P5 $(10.5, 2.0)$, P6 $(-0.5, 0.5)$, P7 $(1.0, 0.5)$ and P8 $(4.0, 0.5)$.

Again one can observe that when τ decreases, the dominant wave number N (for steady state bifurcation) or M (for Hopf bifurcation) increases. When $\tau = 4.5$, the only possible spatial patterns are Turing type (Fig. 4 top row): the constant steady state is stable (see

(a)) if $d_2 = -2.2 > d_{2,1}^S$, while mode-1 Turing patterns emerge if $d_= - 2.5 < d_{2,1}^{lS}$ (see (b) and (c)). When $\tau = 2.0$, From the figures in the middle row of 4, one observes a spatially non-homogeneous mode-2 steady state at $d_2 = -1.35$, a homogeneous pattern at $d_2 = 1$, and a spatially non-homogeneous mode-2 time-periodic pattern at $d_2 = 10.5$ (Fig. 4 middle row). For $\tau = 0.5$, similar sequence of patterns appear with mode-3 (Fig. 4 bottom row). One can also observe the spatially non-homogeneous time-periodic patterns at P5 or P7 are spatially and temporally periodic with expected spatial modes, and they are of "checker-board" type similar to the ones observed in the discrete delay version of spatial memory models in [30, 31].

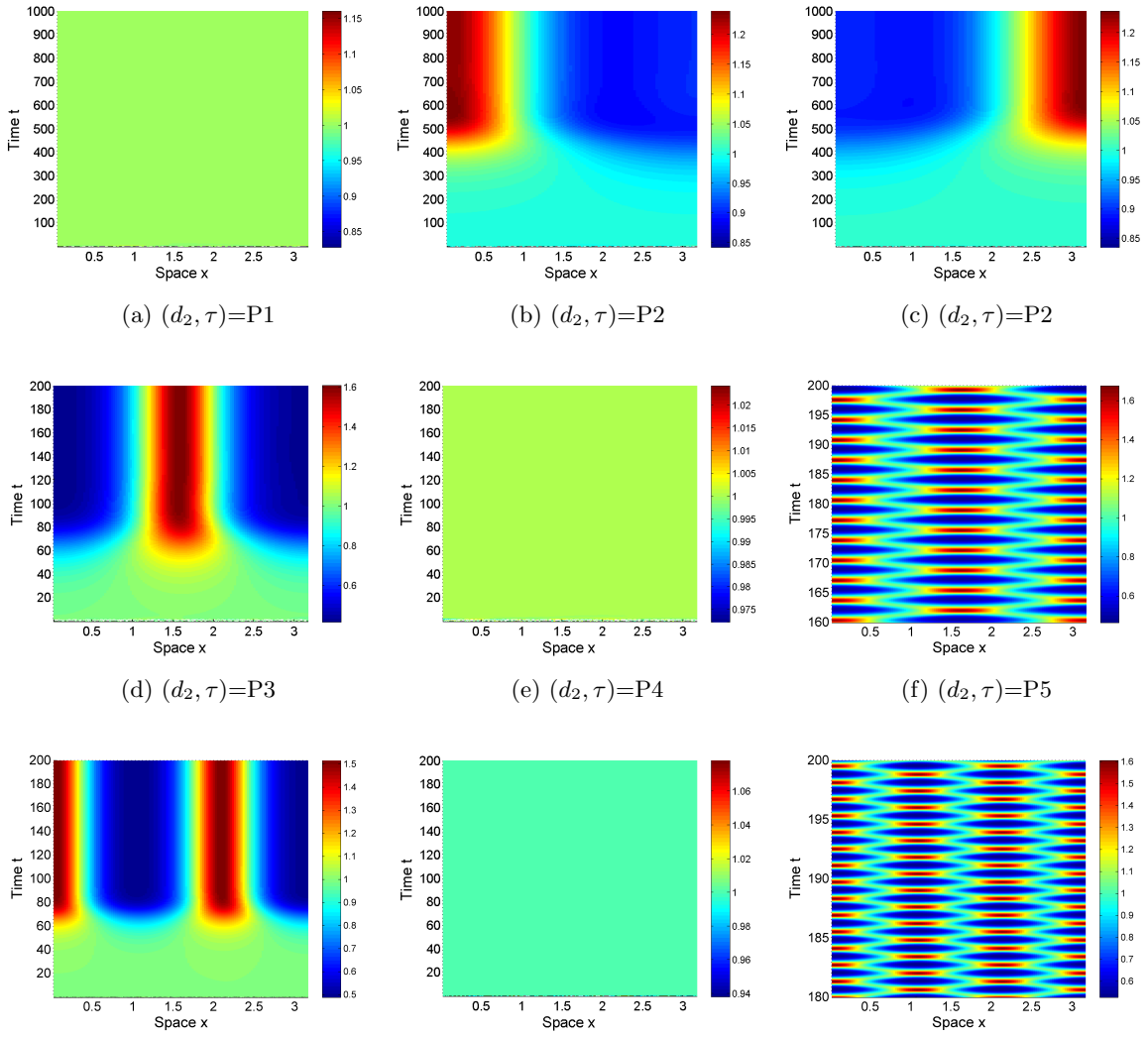

(a) (d_2, τ)=P1 (b) (d_2, τ)=P2 (c) (d_2, τ)=P2

(d) (d_2, τ)=P3 (e) (d_2, τ)=P4 (f) (d_2, τ)=P5

(g) (d_2, τ)=P6 (h) (d_2, τ)=P7 (i) (d_2, τ)=P8

Figure 4: Numerical simulations of system (5.4) when parameters are $d_1 = 0.1$ and $\Omega = (0, \pi)$.

6 Discussion

In the past decade, spatial memory and cognition attracted much attention in the mechanistic modeling of animal movements [10, 24]. A recent strong motivation for the significance of spatial memory in animal movements is the empirical evidence of blue whale migrations presented in Abrahms et al. [1] and discussed in Fagan [8]. Much progress has been made in incorporating spatial cognition or memory implicitly, such as territorial behaviors [22, 23], scent marks [17], taxis-driven pattern formation [26, 27], information gaining via last visit to locations [28], perceptual ranges [9], and delayed resource-driven movement [11]. Among these models, the closest one to ours is the model in Potts and Lewis [27], where they have a drift term depending on the spatially averaged population density at the current time, however, there is no explicit memory because of no delay. Interacting populations were considered in this work, which will be our future efforts. This model was used to study territorial pattern formation in Potts and Lewis [26]. In Schlägel and Lewis [28], information gaining processes were first modeled via last visit to locations. The authors explored the interactions of gained information by past visits with environmental information to shape movement patterns. The resource-driven movement model was proposed in Fagan et al. [9] for studying perceptual ranges and foraging success, and delayed resource-driven movement was proposed in Foss-Grant [11].

We recently proposed a novel diffusive animal movement model with explicit spatial memory [31] by assuming that animals ideally have information gained via their long-distance sights or via communications with their parents and friends in contrast to information gathering via past visits [28]. Based on this recent work, we here formulate a reaction-diffusion scalar equation with a distributed memory-based diffusion term to model the diffusive movement of animals who can memorize the past information. In [31], the memory-based diffusion is related to the memory of a particular moment in the past, which induces the discrete delay. They also mentioned that a distributed delay for memory waning and gaining is more realistic since highly developed animals can remember the historic distribution or clusters of the species in space but these spatial memories are decaying in their brains over time. Such decays may include decreases in intensity and spatial precision [10, 31]. Therefore, this new distributed memory-based model (1.1) provides a more realistic quantitative framework for characterizing complicated memory waning and gaining processes in a relatively simple self-contained way.

The delay kernel plays a vital role in the modeling of distributed delay. In our case, we consider the spatial memory that is related to the memorized information during all the

past time as well as the spatial distribution of the species. Thus, we need to choose proper delay kernels both in space and in time. For the spatial delay kernel, we use the Green's function of diffusion equation which has been employed by many researchers to study the distributed delay effect [5, 12, 42]. The temporal distribution of memory is modeled by weak and strong kernel functions (two special cases of Gamma distribution) which have clear biological meanings. Under such settings, we transform the scalar population model (1.1) with the weak kernel into a two-species system (2.1) in which one of the "species" is the memory of the other one. Similarly, a three-species reaction-diffusion system (2.3) is obtained when the strong kernel is applied to the model. The method to establish the equivalence between the scalar reaction-diffusion equation with distributed delayed diffusion and reaction-diffusion system without delay is very helpful for us to gain a deep understanding of the original delayed model (1.1). Moreover, we proved that the eigenvalue problem of the original scalar equation (1.1) is exactly the same with that of the equivalent systems, which implies the equivalence of the stability of the constant steady state. And the analysis works when the temporal kernel takes Gamma distribution with a larger shape parameter.

As for the findings, surprisingly, Eq. (1.1) with the weak kernel is equivalent to the Keller-Segel chemotaxis model with growth [15, 20, 25, 34], which means that another mechanism for this well-known model is established. In this case, the occurrence of steady state bifurcation of the positive equilibrium can be theoretically proved, thus non-homogeneous steady state exists. Through numerical simulations, we also observed spatially non-homogeneous periodic patterns. However, it is still an open problem to explain some drifting and wandering periodic patterns (see Fig. 2). We conjecture that the reason for these spatially non-homogeneous periodic patterns is that the non-constant steady state undergoes a Hopf bifurcation. For the strong kernel case, the steady state bifurcation and spatially non-homogeneous Hopf bifurcation of the positive equilibrium will lead to spatially non-homogeneous steady state as well as non-homogeneous periodic patterns (see Figs. 4).

In our bifurcation analysis, we use the memory-based diffusion rate d_2 as the focused parameter. Also, we obtain the conditions for pattern formation: $d_2 < d_2^*$ for the weak kernel case and $d_2 \in (-\infty, d_{2,S}^*) \cup (d_{2,H}^*, +\infty)$ for the strong kernel case, which both satisfy $|d_2| > \theta d_1$. Therefore, we can conclude that $|d_2| > \theta d_1$ is a necessary condition for pattern formation in system (1.1). This result is consistent with the necessary condition obtained in [31] for pattern formation of the discrete delayed spatial memory model.

Finally, we want to emphasize the significance of average time delay τ in the diversity of spatial patterns. From the bifurcation diagrams Figs. 1 and 3, we observe that the first

bifurcation curve could be any mode as τ varies. This implies that diverse spatial patterns can emerge, In Fig. 4, it is clear that the spatial structure of the non-homogeneous steady states and periodic solutions is changing for different τ values.

A Appendix

Proof of Theorem 3.3. We apply [6, Theorem 1.7] for the local bifurcation. Fixing $d_1, \tau > 0$, we define a nonlinear mapping $F : \mathbb{R}^+ \times X^2 \to Y^2$ by

$$F(d_2, u, v) = \begin{pmatrix} d_1\Delta u + d_2 div(u\nabla v) + f(u) \\ \\ d_1\Delta v + \frac{1}{\tau}(u - v) \end{pmatrix}. \tag{A.1}$$

It is clear that $F(d_2, \theta, \theta) = 0$ for any $d_2 > 0$. The Fréchet of F with respect to (u, v) is

$$F_{(u,v)}\left(d_{2,n}^w, \theta, \theta\right)[\varphi, \psi] = \begin{pmatrix} d_1\Delta\varphi + d_{2,n}^w\theta\Delta\psi + f'(\theta)\varphi \\ \\ d_1\Delta\psi + \frac{1}{\tau}(\varphi - \psi) \end{pmatrix} := L[\varphi, \psi]. \tag{A.2}$$

Step 1. First we determine the null space of L. From Lemma 3.1, we have $D_n(d_{2,s}^w) = 0$ so $\mu = 0$ is an eigenvalue of J_n^w defined in (3.3) thus also an eigenvalue of (3.2) and there exists $q = (\varphi, \psi)^T = (1, h_n)\phi_n \in \mathcal{N}(L)$. Moreover as $T_n(d_{2,s}^w) > 0$, $\mu = 0$ is a simple eigenvalue of J_n^w; and since λ_n is a simple eigenvalue of (1.5), and $d_{2,n}^w \neq d_{2,k}^w$ for any $k \in \mathbb{N}$ and $k \neq n$, then $\mu = 0$ is as simple of L and

$$\mathcal{N}(L) = \text{Span}\left\{q = (1, h_n)\phi_n\right\},$$

with $h_n = 1/(d_1\lambda_n\tau + 1)$, thus $\dim\left(\mathcal{N}(L)\right) = 1$.

Step 2. We next consider the range space $\mathcal{R}(L)$ of L. We can verify that $\mathcal{R}(L)$ is given by $\{(f_1, f_2) \in Y^2 : \langle q^*, (f_1, f_2)\rangle = 0\}$ where $q^* \in \mathcal{N}(L^*)$ and L^* is the adjoint operator of L and defined by

$$L^*[\varphi, \psi] = \begin{pmatrix} d_1\Delta\varphi + f'(\theta)\varphi + \frac{1}{\tau}\psi \\ \\ d_1\Delta\psi + d_{2,n}^w\theta\Delta\varphi - \frac{1}{\tau}\psi \end{pmatrix}. \tag{A.3}$$

Since $\mathcal{N}(L^*) = \text{Span}\left\{q^* = (1, r_n)^T\phi_n\right\}$, where $r_n = \tau(d_1\lambda_n - f'(\theta))$. We obtain

$$\mathcal{R}(L) = \left\{(f_1, f_2) \in Y^2 : \int_\Omega (f_1 + r_n f_2)\,\phi_n dx = 0\right\},$$

and $\text{codim}\left(\mathcal{R}(L)\right) = 1$.

Step 3. We show that $F_{d_2(u,v)}(d_{2,n}^w, \theta, \theta)[q] \notin \mathcal{R}(L)$. From (A.1), we have

$$F_{d_2(u,v)}\left(d_{2,n}^w, \theta, \theta\right)[q] = (\theta h_n\Delta\phi_n, 0)^T = (-\theta\lambda_n h_n\phi_n, 0)^T. \tag{A.4}$$

Since

$$\int_\Omega \left(-\theta\lambda_n h_n \phi_n + 0\right)\phi_n dx = -\theta\lambda_n h_n \int_\Omega \phi_n^2 dx < 0,$$

thus $F_{d_2(u,v)}\left(d_{2,n}^w, \theta, \theta\right)[q] \notin \mathcal{R}(L)$ by the definition of $\mathcal{R}(L)$. From Step 1, 2 and 3, now we can apply [6, Theorem 1.7] to obtain part (i).

Step 4. Now we consider the bifurcation direction and stability of the bifurcating solutions in Γ_n. To obtain more detailed information of the bifurcation, we use one-dimensional domain $\Omega = (0, l\pi)$. In this case, it is known that $\phi_n = \cos(nx/l)$ and $\lambda_n = n^2/l^2$, so that $q = (1, h_n)^T \cos(nx/l)$. From [29], we have

$$d'_{2,n}(0) = -\frac{\langle l, F_{(u,v)(u,v)}(d_{2,n}^w, \theta, \theta)[q, q]\rangle}{2\langle l, F_{d_2(u,v)}(d_{2,n}^w, \theta, \theta)[q]\rangle},$$

where $l \in Y$ satisfies $\mathcal{N}(l) = \mathcal{R}(L)$ and can be calculated as

$$\langle l, (f_1, f_2)\rangle = \int_0^{l\pi} (f_1 + r_n f_2)\cos\left(\frac{nx}{l}\right) dx.$$

By (A.4) and the definition of l, we have

$$\left\langle l,\ F_{d_2(u,v)}\left(d_{2,n}^w, \theta, \theta\right)[q]\right\rangle = -\lambda_n h_n \theta \int_0^{l\pi} \cos^2\left(\frac{nx}{l}\right) dx = -\frac{\lambda_n h_n \theta l\pi}{2}.$$

From (A.1), it can be obtained that

$$F_{(u,v)(u,v)}(d_2, u, v)[\varphi, \psi][\varphi, \psi] = \left(2d_2\varphi'\psi' + 2d_2\varphi\psi'' + f''(u)\varphi^2, 0\right)^T. \tag{A.5}$$

This implies that

$$F_{(u,v)(u,v)}\left(d_{2,n}^w, \theta, \theta\right)[q, q] = \left(\frac{f''(\theta)}{2} + \left(\frac{f''(\theta)}{2} - 2d_{2,n}^w h_n \lambda_n\right)\cos\left(\frac{2nx}{l}\right), 0\right)^T, \tag{A.6}$$

and thus

$$\begin{aligned}&\left\langle l,\ F_{(u,v)(u,v)}\left(d_{2,n}^w, \theta, \theta\right)[q, q]\right\rangle \\ &= \int_0^{l\pi} \left(\frac{f''(\theta)}{2} + \left(\frac{f''(\theta)}{2} - 2d_{2,n}^w h_n \lambda_n\right)\cos\left(\frac{2nx}{l}\right)\right)\cos\left(\frac{nx}{l}\right) dx = 0.\end{aligned}$$

Therefore $d'_{2,n}(0) = 0$.

Next we calculate $d''_{2,n}(0)$ to determine the bifurcation direction by modifying the calculation in [14]. From [29], $d''_{2,n}(0)$ takes the form:

$$d''_{2,n}(0) = -\frac{\left\langle l,\ F_{(u,v)(u,v)(u,v)}\left(d_{2,n}^w, \theta, \theta\right)[q, q, q]\right\rangle + 3\left\langle l,\ F_{(u,v)(u,v)}\left(d_{2,n}^w, \theta, \theta\right)[q, \Theta]\right\rangle}{3\left\langle l,\ F_{d_2(u,v)}(d_{2,n}^w, \theta, \theta)[q]\right\rangle},$$

where $\Theta = (\Theta_1, \Theta_2)$ is the unique solution of

$$F_{(u,v)(u,v)}\left(d_{2,n}^w, \theta, \theta\right)[q, q] + F_{(u,v)}\left(d_{2,n}^w, \theta, \theta\right)[\Theta] = 0. \tag{A.7}$$

From (A.5), we have

$$F_{(u,v)(u,v)(u,v)}\left(d_2,u,v\right)[\varphi,\psi][\varphi,\psi][\varphi,\psi]=(f'''(u)\varphi^3,0)^T,$$

thus

$$\langle l,F_{(u,v)(u,v)(u,v)}\left(d_{2,n}^w,\theta,\theta\right)[q,q,q]\rangle=\int_0^{l\pi}f'''(\theta)\cos^4\left(\frac{nx}{l}\right)dx=\frac{3l\pi}{8}f'''(\theta). \tag{A.8}$$

In the following, we show the calculation of $\left\langle l,\ F_{(u,v)(u,v)}\left(d_{2,n}^w,\theta,\theta\right)[q,\Theta]\right\rangle$. By (A.6) and (A.7), we may assume $\Theta=(\Theta_1,\Theta_2)$ has the following form

$$\Theta_1=\Theta_1^0+\Theta_1^2\cos\left(\frac{2nx}{l}\right),\ \Theta_2=\Theta_2^0+\Theta_2^2\cos\left(\frac{2nx}{l}\right), \tag{A.9}$$

since $F_{(u,v)(u,v)}\left(d_{2,n}^w,\theta,\theta\right)$ consists of only constant and $\cos\left(\frac{2nx}{l}\right)$ terms. Substituting (A.9) into (A.7), we obtain

$$\begin{aligned}&\begin{pmatrix}-4d_1\lambda_n\Theta_1^2\cos\left(\frac{2nx}{l}\right)-4d_{2,n}^w\theta\lambda_n\Theta_2^2\cos\left(\frac{2nx}{l}\right)+f'(\theta)\left(\Theta_1^0+\Theta_1^2\cos\left(\frac{2nx}{l}\right)\right)\\ -4d_1\lambda_n\Theta_2^2\cos\left(\frac{2nx}{l}\right)+\frac{1}{\tau}[\Theta_1^0-\Theta_2^0+(\Theta_1^2-\Theta_2^2)\cos\left(\frac{2nx}{l}\right)]\end{pmatrix}\\ &=-\left(\frac{f''(\theta)}{2}+\left(\frac{f''(\theta)}{2}-2d_{2,n}^w\lambda_nh_n\right)\cos\left(\frac{2nx}{l}\right),0\right)^T.\end{aligned} \tag{A.10}$$

Form Eq. (A.10), we can solve Θ as in (3.10). Thus, we obtain

$$\begin{aligned}&\left\langle l,\ F_{(u,v)(u,v)}\left(d_{2,n}^w,\theta,\theta\right)[q,\Theta]\right\rangle\\ =&2d_{2,n}^w\lambda_n(\Theta_2^2+h_n\Theta_1^2)\int_0^{l\pi}\sin\left(\frac{2nx}{l}\right)\sin\left(\frac{nx}{l}\right)\cos\left(\frac{nx}{l}\right)dx\\ &+\left(f''(\theta)-d_{2,n}^w\lambda_nh_n\right)\Theta_1^0\int_0^{l\pi}\cos^2\left(\frac{nx}{l}\right)dx\\ &+\left(f''(\theta)\Theta_1^2-d_{2,n}^w\lambda_nh_n\Theta_1^2-4d_{2,n}^w\lambda_n\Theta_2^2\right)\Theta_1^2\int_0^{l\pi}\cos\left(\frac{2nx}{l}\right)\cos^2\left(\frac{nx}{l}\right)dx\\ =&\frac{l\pi}{2}d_{2,n}^w(\Theta_2^2+h_n\Theta_1^2\lambda_n)+\frac{l\pi}{2}\left(f''(\theta)-d_{2,n}^w\lambda_nh_n\right)\Theta_1^0+\frac{l\pi}{4}(f''(\theta)\Theta_1^2-4d_{2,n}^w\lambda_n\Theta_2^2-d_{2,n}^w\lambda_nh_n\Theta_1^2).\end{aligned}$$

Using all above we obtain $d_{2,n}''(0)$ in Eq. (3.9).

Step 5. By applying Corollary 1.13 and Theorem 1.16 in [7] or Theorem 5.4 in [18], the stability of the bifurcating non-constant steady states can be determined by the sign of $\mu(s)$ which satisfies

$$\lim_{s\to0}\frac{-sd_{2,n}'(s)m'(d_{2,n}^w)}{\mu(s)}=1, \tag{A.11}$$

where $m(d_2)$ and $\mu(s)$ are the eigenvalues defined as

$$F_{(u,v)}(d_2,\theta,\theta)[\varphi(d_2),\psi(d_2)]=m(d_2)K[\varphi(d_2),\psi(d_2)],\quad\text{for } d_2\in(d_{2,n}^w-\epsilon,d_{2,n}^w+\epsilon),$$

$$F_{(u,v)}(d_{2,n}(s),U_n(s),V_n(s))[\Lambda(s),\Phi(s)]=\mu(s)K[\Lambda(s),\Phi(s)],\quad\text{for } s\in(-\delta,\delta),$$

with $K : X \to Y$ is the inclusion map $K(u) = u$, $m\left(d_{2,n}^w\right) = \mu(0) = 0$ and $\left(\varphi\left(d_{2,n}^w\right), \psi\left(d_{2,n}^w\right)\right) = (\Lambda(0), \Phi(0)) = (1, h_n)\cos\left(\frac{nx}{l}\right)$.

Now consider the bifurcation at $d_2 = d_{2,N}^w = d_2^*$. From Lemma 3.1, (θ, θ) is stable and $m(d_2) < 0$ when $d_2 > d_{2,N}^w$, and it is unstable and $m(d_2) > 0$ when $d_2 < d_{2,N}^w$. One can calculate that

$$m(d_2) = \frac{-T_N + \sqrt{T_N^2 - 4D_N}}{2},$$

where T_N, D_N are defined in (3.5), and this implies that $m'(d_{2,N}^w) = -\theta\lambda_N/(T_N\tau) < 0$. If $d_{2,N}''(0) < 0$, then $d_{2,N}'(s) < 0$ for $s \in (0, \delta)$ and $d_{2,N}'(s) > 0$ for $s \in (-\delta, 0)$. Hence $-sd_2'(s)m'(d_{2,N}^w) < 0$ for $s \in (-\delta, \delta)\backslash\{0\}$, and consequently $\mu(s) < 0$ by(A.11) and the bifurcating solutions are locally asymptotically stable. Similarly when $d_{2,N}''(0) > 0$, the bifurcating solutions are unstable. For any other bifurcation at $d_2 = d_{2,n}^w < d_2^*$, the trivial solution (θ, θ) is already unstable at the bifurcation point, hence all bifurcating solutions are also unstable. □

References

[1] B. Abrahms, E. L. Hazen, E. O. Aikens, M. S. Savoca, J. A. Goldbogen, S. J. Bograd, M. G. Jacox, L. M. Irvine, D. M. Palacios, and B. R. Mate. Memory and resource tracking drive blue whale migrations. *Proc. Natl. Acad. Sci.*, 116(12):5582–5587, 2019.

[2] H. Amann. Hopf bifurcation in quasilinear reaction-diffusion systems. In *Delay differential equations and dynamical systems (Claremont, CA, 1990)*, volume 1475 of *Lecture Notes in Math.*, pages 53–63. Springer, Berlin, 1991.

[3] N. Bellomo, A. Bellouquid, Y. S. Tao, and M. Winkler. Toward a mathematical theory of Keller-Segel models of pattern formation in biological tissues. *Math. Models Methods Appl. Sci.*, 25(9):1663–1763, 2015.

[4] N. F. Britton. Spatial structures and periodic travelling waves in an integro-differential reaction-diffusion population model. *SIAM J. Appl. Math.*, 50(6):1663–1688, 1990.

[5] S. S. Chen and J. S. Yu. Stability analysis of a reaction-diffusion equation with spatiotemporal delay and Dirichlet boundary condition. *J. Dynam. Differential Equations*, 28(3-4):857–866, 2016.

[6] M. G. Crandall and P. H. Rabinowitz. Bifurcation from simple eigenvalues. *J. Functional Analysis*, 8:321–340, 1971.

[7] M. G. Crandall and P. H. Rabinowitz. Bifurcation, perturbation of simple eigenvalues and linearized stability. *Arch. Rational Mech. Anal.*, 52:161–180, 1973.

[8] W. F. Fagan. Migrating whales depend on memory to exploit reliable resources. *Proc. Natl. Acad. Sci.*, 116(12):5217–5219, 2019.

[9] W. F. Fagan, E. Gurarie, S. Bewick, A. Howard, R. S. Cantrell, and C. Cosner. Perceptual ranges, information gathering, and foraging success in dynamic landscapes. *Am. Nat.*, 189(5):474–489, 2017.

[10] W. F. Fagan, M. A. Lewis, M. Auger-Méthé, T. Avgar, S. Benhamou, G. Breed, U. E. LaDage, L.and Schlägel, W. W. Tang, Y. P. Papastamatiou, J. Forester, and T. Mueller. Spatial memory and animal movement. *Ecology Letters*, 16(10):1316–1329, 2013.

[11] A. P. Foss-Grant. *Quantitative challenges in ecology: competition, migration, and social learning*. PhD thesis, 2017.

[12] S. A. Gourley and J. W.-H. So. Dynamics of a food-limited population model incorporating nonlocal delays on a finite domain. *J. Math. Biol.*, 44(1):49–78, 2002.

[13] T. Hillen and K. J. Painter. A user's guide to PDE models for chemotaxis. *J. Math. Biol.*, 58(1-2):183–217, 2009.

[14] J. Y. Jin, J. P. Shi, J. J. Wei, and F. Q. Yi. Bifurcations of patterned solutions in the diffusive Lengyel-Epstein system of CIMA chemical reactions. *Rocky Mountain J. Math.*, 43(5):1637–1674, 2013.

[15] E. F. Keller and L. A. Segel. Initiation of slime mold aggregation viewed as an instability. *Journal of Theoretical Biology*, 26(3):399–415, 1970.

[16] K. Kuto, K. Osaki, T. Sakurai, and T. Tsujikawa. Spatial pattern formation in a chemotaxis-diffusion-growth model. *Phys. D*, 241(19):1629–1639, 2012.

[17] M. A. Lewis and J. D. Murray. Modelling territoriality and wolf–deer interactions. *Nature*, 366(6457):738–740, 1993.

[18] P. Liu and J. P. Shi. Bifurcation of positive solutions to scalar reaction-diffusion equations with nonlinear boundary condition. *J. Differential Equations*, 264(1):425–454, 2018.

[19] P. Liu, J. P. Shi, and Z. A. Wang. Pattern formation of the attraction-repulsion Keller-Segel system. *Discrete Contin. Dyn. Syst. Ser. B*, 18(10):2597–2625, 2013.

[20] M. J. Ma and Z. A. Wang. Global bifurcation and stability of steady states for a reaction-diffusion-chemotaxis model with volume-filling effect. *Nonlinearity*, 28(8):2639–2660, 2015.

[21] M. Mimura and T. Tsujikawa. Aggregating pattern dynamics in a chemotaxis model including growth. *Physica A: Statistical Mechanics and its Applications*, 230(3-4):499–543, 1996.

[22] P. R. Moorcroft, M. A. Lewis, and R. L. Crabtree. Home range analysis using a mechanistic home range model. *Ecology*, 80(5):1656–1665, 1999.

[23] P. R. Moorcroft, P. Moorcroft, and M. A. Lewis. *Mechanistic home range analysis*. Princeton University Press, 2006.

[24] J. M. Morales, P. R. Moorcroft, J. Matthiopoulos, J. L. Frair, J. G. Kie, R. A. Powell, E. H. Merrill, and D. T. Haydon. Building the bridge between animal movement and population dynamics. *Philosophical Transactions of the Royal Society B: Biological Sciences*, 365(1550):2289–2301, 2010.

[25] K. J. Painter and T. Hillen. Spatio-temporal chaos in a chemotaxis model. *Physica D: Nonlinear Phenomena*, 240(4-5):363–375, 2011.

[26] J. R. Potts and M. A. Lewis. How memory of direct animal interactions can lead to territorial pattern formation. *Journal of the Royal Society Interface*, 13(118):20160059, 2016.

[27] J. R. Potts and M. A. Lewis. Spatial memory and taxis-driven pattern formation in model ecosystems. *Bull. Math. Biol.*, 81(7):2725–2747, 2019.

[28] U. E. Schlägel and M. A. Lewis. Detecting effects of spatial memory and dynamic information on animal movement decisions. *Methods in Ecology and Evolution*, 5(11):1236–1246, 2014.

[29] J. P. Shi. Persistence and bifurcation of degenerate solutions. *J. Funct. Anal.*, 169(2):494–531, 1999.

[30] J. P. Shi, C. C. Wang, and H. Wang. Diffusive spatial movement with memory and maturation delays. *Nonlinearity*, 32(9):3188–3208, 2019.

[31] J. P. Shi, C. C. Wang, H. Wang, and X. P. Yan. Diffusive spatial movement with memory. *J. Dynam. Differential Equations*, 2020 (to appear).

[32] J. P. Shi and X. F. Wang. On global bifurcation for quasilinear elliptic systems on bounded domains. *J. Differential Equations*, 246(7):2788–2812, 2009.

[33] Y. S. Tao. Global dynamics in a higher-dimensional repulsion chemotaxis model with nonlinear sensitivity. *Discrete Contin. Dyn. Syst. Ser. B*, 18(10):2705–2722, 2013.

[34] J. I. Tello and M. Winkler. A chemotaxis system with logistic source. *Comm. Partial Differential Equations*, 32(4-6):849–877, 2007.

[35] A. M. Turing. The chemical basis of morphogenesis. *Philos. Trans. Roy. Soc. London Ser. B*, 237(641):37–72, 1952.

[36] Z. A. Wang and K. Zhao. Global dynamics and diffusion limit of a one-dimensional repulsive chemotaxis model. *Commun. Pure Appl. Anal.*, 12(6):3027–3046, 2013.

[37] M. Winkler. Boundedness in the higher-dimensional parabolic-parabolic chemotaxis system with logistic source. *Comm. Partial Differential Equations*, 35(8):1516–1537, 2010.

[38] M. Winkler. Global asymptotic stability of constant equilibria in a fully parabolic chemotaxis system with strong logistic dampening. *J. Differential Equations*, 257(4):1056–1077, 2014.

[39] M. Winkler. How far can chemotactic cross-diffusion enforce exceeding carrying capacities? *J. Nonlinear Sci.*, 24(5):809–855, 2014.

[40] M. Winkler. Emergence of large population densities despite logistic growth restrictions in fully parabolic chemotaxis systems. *Discrete Contin. Dyn. Syst. Ser. B*, 22(7):2777–2793, 2017.

[41] W. J. Zuo and J. P. Shi. Existence and stability of steady state solutions of reaction-diffusion equations with nonlocal delay effect. *Submitted*, 2020.

[42] W. J. Zuo and Y. L. Song. Stability and bifurcation analysis of a reaction-diffusion equation with spatio-temporal delay. *J. Math. Anal. Appl.*, 430(1):243–261, 2015.